

# REPORT DOCUMENTATION PAGE

Form Approved  
OMB NO. 0704-0188

Public reporting burden for this collection of information is estimated to average 1 hour per response, including the time for reviewing instructions, searching existing data sources, gathering and maintaining the data needed, and completing and reviewing the collection of information. Send comment regarding this burden estimate or any other aspect of this collection of information, including suggestions for reducing this burden, to Washington Headquarters Services, Directorate for Information Operations and Reports, 1215 Jefferson Davis Highway, Suite 1204, Arlington, VA 22202-4302, and to the Office of Management and Budget, Paperwork Reduction Project (0704-0188), Washington, DC 20503.

|   |   |  |   |  |
|---|---|--|---|--|
| 1. AGENCY USE ONLY (Leave blank)  |   | 2. REPORT DATE<br>January 1999             | 3. REPORT TYPE AND DATES COVERED<br>Final Report                              |  |
| 4. TITLE AND SUBTITLE<br>The Effects of Hurricane Nora on eomorphic Characteristics of Yuma Wash, Yuma Proving Ground, Arizona  |   |  | 5. FUNDING NUMBERS<br><br>DAAG55-98-1-0037                                    |  |
| 6. AUTHOR(S)<br>Ellen Wohl<br>David Merritt   |   |  |   |  |
| 7. PERFORMING ORGANIZATION NAMES(S) AND ADDRESS(ES)<br><br>Dept. of Earth Resources<br>Colorado State University<br>Ft. Collins, CO 80523   |   |  | 8. PERFORMING ORGANIZATION<br>REPORT NUMBER                                   |  |
| 9. SPONSORING / MONITORING AGENCY NAME(S) AND ADDRESS(ES)<br><br>U.S. Army Research Office<br>P.O. Box 12211<br>Research Triangle Park, NC 27709-2211   |   |  | 10. SPONSORING / MONITORING<br>AGENCY REPORT NUMBER<br><br>ARO 38707.1- EV-II |  |
| 11. SUPPLEMENTARY NOTES<br>The views, opinions and/or findings contained in this report are those of the author(s) and should not be construed as an official Department of the Army position, policy or decision, unless so designated by other documentation.   |   |  |   |  |
| 12a. DISTRIBUTION / AVAILABILITY STATEMENT<br><br>Approved for public release; distribution unlimited.  |   |  | 12 b. DISTRIBUTION CODE   |  |
| 13. ABSTRACT (Maximum 200 words)<br><br>A baseline survey of Yuma Wash conducted in 1995 was used to assess channel changes associated with flooding from Hurricane Nora in September 1997. Repeat surveys conducted in January 1998 were compared to the 1995 survey to measure areas of cross-sectional scour and fill, net change in channel area, and change in thalweg depth along the channel. One-dimensional hydraulics modeling was used to estimate flood peak discharge and hydraulic variables. Statistical analyses were used to determine which physical drainage basin and channel attributes, and which hydraulic variables, best explained observed changes in channel geometry. September 1997 flood peak discharge varied from 16 to 237 m <sup>3</sup> /s, increasing rapidly downstream. Older high-water marks (probably from 1972) recorded a peak discharge of 1280 m <sup>3</sup> /s. Channel change ranged from a maximum of -10 m <sup>2</sup> of degradation to 33 m <sup>2</sup> of aggradation. Cross sections with wider valleys, numerous multiple channels, and less vegetation aggraded, whereas cross sections in narrower valleys with fewer channels and more vegetation degraded. Cross sections with greater maximum flow depth also aggraded; those with lower flow depth degraded. |   |  |   |  |
| 14. SUBJECT TERMS<br><br>channel change, fluvial geomorphology, flood, Yuma Wash, Yuma Proving Grounds  |   |  | 15. NUMBER OF PAGES<br>36   |  |
|   |   |  | 16. PRICE CODE  |  |
| 17. SECURITY CLASSIFICATION<br>OR REPORT  | 18. SECURITY CLASSIFICATION<br>OF THIS PAGE | 19. SECURITY CLASSIFICATION<br>OF ABSTRACT | 20. LIMITATION OF ABSTRACT  |  |

**The Effects of Hurricane Nora on Geomorphic  
Characteristics of Yuma Wash,  
Yuma Proving Ground, Arizona**

Final Report Submitted to The United States Department of Defense  
Grant Number: DAAG55-98-1-0037

January 1999

Submitted by

David M. Merritt and Ellen E. Wohl  
Department of Earth Resources  
Colorado State University  
Fort Collins, CO

19990706 050

## Table of Contents

|  |    |
|--|----|
| Purpose .....  | 1  |
| Introduction .....   | 2  |
| <i>Site Description</i> .....  | 2  |
| <i>Hurricane Nora</i> .....  | 5  |
| Methods .....  | 8  |
| <i>Post Hurricane Nora Re-Surveys</i> .....                                    | 8  |
| <i>Hydraulics Modeling</i> .....   | 9  |
| <i>Calculations of Channel Change</i> .....                                    | 10 |
| <i>Spatial Scale Controls on Channel Change</i> .....                          | 14 |
| <i>Classification of Cross Sections Based on Physical Attributes</i> .....     | 15 |
| Results and Discussion .....   | 16 |
| <i>Hydraulics Modeling and Slope-Area Flow Estimates</i> .....                 | 16 |
| <i>Channel Change</i> .....  | 23 |
| <i>Spatial Scale Controls on Channel Change</i> .....                          | 28 |
| <i>Classification of Cross Sections Based on Physical Attributes</i> .....     | 28 |
| Conclusions .....  | 31 |
| <i>Implications for Land Management at Yuma Proving Ground</i> .....           | 32 |
| Literature Cited .....   | 34 |
| Appendix I: Re-Surveyed Cross Sections, Yuma Wash .....                        | 37 |
| Appendix II: Paired Photographs of Re-surveyed Cross Sections, Yuma Wash ..... | 43 |
| Appendix III: Grain Size Distributions, Yuma Wash .....                        | 53 |
| Appendix IV: Data .....  | 55 |
| Appendix V: SAS Statistics Code and Data Files .....                           | 59 |

## Purpose

The purpose of this study is to examine the effects of floods associated with Hurricane Nora on the geomorphic characteristics of Yuma Wash, southwestern Arizona. In this investigation, we assess the flood-related geomorphic change that occurred in September 1997 in Yuma Wash, using analysis of pre and post hurricane field survey data. Flow and flood hydraulics associated with flooding in Yuma Wash are estimated using step backwater modeling as well as slope-area equations. The magnitude of the storms associated with Hurricane Nora are compared to historic records through the use of meteorological data gathered by remote weather stations located at Yuma Wash and long-term precipitation records from a weather station located in Yuma Proving Ground (YPG). We then determine which physical attributes of Yuma Wash best explain the measured channel changes. Spatial controls on the observed channel changes are then examined through analyzing basin, reach, and cross section scale attributes.

This study was funded by the Department of Defense under the Legacy Resource Management Program. The goals of the LRMP are to establish a management program to identify and manage geophysical resources on lands owned by the Department of Defense and to develop programs to restore and rehabilitate altered or degraded habitats. This project contributes to these goals in that it utilizes baseline data gathered prior to Hurricane Nora to assess flood related geomorphic change within the wash. In this study, analytical modeling is used to estimate the magnitude of the Hurricane Nora flood in Yuma Wash. Furthermore, we interpret the geomorphic changes associated with such an event in the context of the spatial controls of channel change. Climate change, random variability, and land-use impacts are among the factors hypothesized to control gully and arroyo formation in ephemeral stream systems throughout the Southwest (Cooke and Reeves 1976). The latter of these is the only factor that may be controlled through modifications to land-use patterns. Understanding normal erosional and depositional processes in ephemeral channels during high magnitude floods may provide data which will aid in management decisions. Through investigations that examine the responses of ephemeral channels to natural disturbances such as flooding, an understanding of the potential effects of various human activities within these systems may be developed.

Data used in this study are from a variety of sources. Baseline data are from field surveys conducted by Ayres Associates in 1995 as a part of 'Geomorphic, Hydrologic, and Vegetation Characterization and Base-Line Conditions of Yuma Wash, Yuma Proving Grounds, Arizona' (Ayres Associates 1996). Drainage area, elevations of cross section endpoints above mean sea level, and distances between cross sections used in this study were calculated by Ayres Associates. Meteorologic data are from remote weather stations established as a part of the base-line study. These unpublished data are used with the permission of J.D. Stednick at Colorado State University. Long-term precipitation records were obtained from the NCDC Summary of the Day database from the National Oceanic and Atmospheric Administration (NOAA 1998). All other data presented in this report are from field visits to Yuma Wash January 25 - 29, 1998 (Appendix IV).

## Introduction

### *Site Description*

Yuma Wash is an ephemeral, sand-bed stream located in the Lower Sonoran Desert in southwestern Arizona (Figure 1). The wash is approximately 27 km long and 8 km wide, drains an area of 186 km<sup>2</sup>, and is a tributary of the Colorado River. A majority of the wash lies within the 3400 km<sup>2</sup> Yuma Proving Ground military test facility and is managed by the U.S. Department of Defense. A small portion of the lower wash bordering the Colorado River is managed by the U.S. Fish and Wildlife Service and is located within Imperial National Wildlife Refuge.

Historically, most military activities took place on the desert terrain surrounding the alluvial bottomlands. These upland areas within YPG are characterized by sparse vegetation and delicate desert pavement surfaces which require an extremely long period of time to recover from mechanical disturbances. In an effort to decrease the long-term impacts of military activities to the upland areas within YPG, activities have become more concentrated in alluvial valley bottoms, which are more resilient to disturbance. It is unknown what effects this increase in activity may have on sediment supply and sediment transport within wash systems, and what long and short-term consequences changes in these factors may have on channel morphology downstream.

In 1996, as a part of the Legacy Resource Management Program, the Department of Defense initiated a baseline study of the geologic, geophysical, and biological resources within Yuma Proving Ground (YPG). The portion of this baseline study most relevant to the current work included the establishment of 22 cross-sections which were surveyed and monumented by Ayres Associates within the main stem of Yuma Wash (Ayres Associates 1996). Examining channel change through re-surveys of a subset of these cross sections forms the basis of this study. As a part of the baseline study of Yuma Wash, Ayres Associates divided the wash into four distinct reaches, characterizing reaches based on valley physiography (primarily valley width). Longitudinally from the headwaters of the Yuma Wash to its terminus, the wash widens from a relatively narrow valley (~50 m wide) with a single dominant channel furthest upstream, to a wide multiple channeled valley bottom exceeding 450 m where the wash enters the Colorado River. The upper reaches of the wash are incised into andesitic bedrock and are laterally confined on one or both sides, whereas the lower reaches consist of channels formed in coarse unconsolidated alluvium with some exposure of basalt and andesite (Wilson 1960).

Yuma Wash is a braided stream characterized by very high width to depth ratios and little to no true floodplain development. There are, however, well developed sets of Holocene terraces within the wash. These terraces are not subject to flooding under current climatic regimes (Graf 1987). The wash is bordered on its north and western edge by the Trigo Mountains and on its east by the Chocolate Mountains. These mountains are comprised of Tertiary agglomerate andesites (volcanic origin), with some areas of exposed Mesozoic schists in

the lower reaches of the basin and a small exposure of Quaternary basalt in the intermediate reaches of the basin (Wilson 1960). The watershed of the wash is oriented north to south and descends 371 m from the base of Mohave Peak (elevation 427 m) to its confluence with the

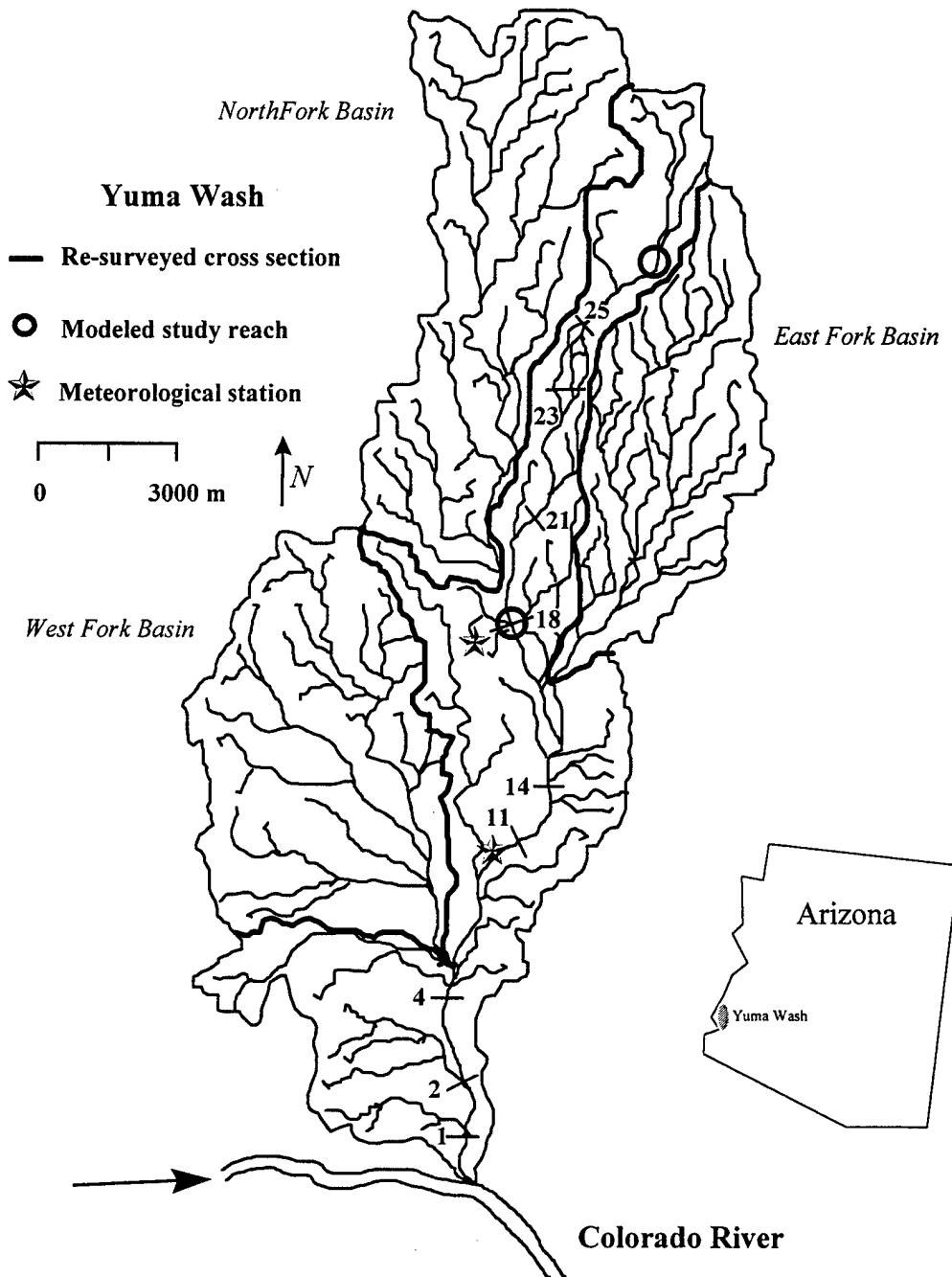


Figure 1. Study area map of Yuma Wash. Locations of re-surveyed cross sections, remote weather stations, and hydraulics modeling reaches are indicated. Base map redrawn with modification from Ayres Associates (1996).

Colorado River (elevation 56 m). All elevations in this report are given in meters above mean sea level. There are four sub-basins within Yuma Wash: the main stem of Yuma Wash (66 km<sup>2</sup>), the North Fork (43 km<sup>2</sup>), the West Fork (43 km<sup>2</sup>), and the East Fork (34 km<sup>2</sup>) Basins. The landscape in the valley surrounding the wash is sparsely vegetated by desert scrub with well developed desert pavement in some areas. As is typical of most ephemeral streams throughout the southwestern U.S. and other arid regions worldwide, the Yuma Wash is sand dominated and is characterized by long periods of no flow punctuated by short periods of high flow, unstable boundary conditions, and high sediment loads when flooding does occur.

Although the wash is sparsely vegetated, lowland areas/wash bottoms support the lushest and most biologically diverse vegetation within YPG and throughout the region (Hermann Zillgens Associates 1992). Vegetation cover measured in this study averaged 31% within Yuma Wash. Vegetation cover in upland areas within YPG is approximately 1-5% (Ayres Associates 1996). Along the valley bottom where flow is ephemeral, dominant vegetation is composed primarily of xeric woody species and phreatophytic vegetation such as brittlebush, ironwood, creosote bush, blue palo verde, smoke-bush, honey mesquite, and catclaw acacia. Vegetation within the channel plays a significant role in sediment processes within the wash, as will be discussed below.

The climate of the region is arid, receiving an annual average of 93 mm of precipitation (NOAA 1998). In ephemeral systems such as Yuma Wash, all fluvial activity results from precipitation. The duration, intensity, and frequency of precipitation of various magnitudes determines the intensity and periodicity of flooding in valley bottoms. Whereas channel morphology in perennial streams has been shown to be adjusted to some average flow condition, such as bankfull flow or effective discharge, channel morphology along ephemeral streams may be a product of less common precipitation-related-events which generate the large flows.

It has been hypothesized that although high volumes of sediment are transported during relatively small but frequent flood events, larger less frequent floods are responsible for channel form (Kochel 1988). Streams that experience the most dramatic change in channel form during high magnitude, threshold-crossing flows typically have flashy hydrographs, steep gradients, coarse bedload, and channels conducive to highly turbulent flow (Kochel 1988). Other investigations have suggested that channel morphology on ephemeral streams is more closely related to smaller, more frequent floods than to less frequent 'threshold-crossing' flows. Begin and Inbar (1984) found that the grain size of bed materials in ephemeral streams in Israel were more closely associated with more frequent flows than with large, rare floods. As is shown in this study, large and small flows perform distinct geomorphic functions in ephemeral channels. Channel morphology is likely determined by a combination of small annual flows and less frequent catastrophic flooding.

Because of the high infiltration rate typical of desert soils, surface flow requires intense precipitation to occur for a duration sufficient for floodwater to pool and propagate downstream before infiltrating into the coarse alluvium of the stream bed. Even during lower intensity

rainfall, runoff may be very rapid in arid environments due to the predominance of exposed bedrock surfaces in desert regions (Schick 1988). Nonetheless, flow is largely determined by the characteristics of the storm (intensity and duration ) in a given watershed. As a consequence, the processes that generate rainstorms in the lower Sonoran Desert influence the characteristics of precipitation, and subsequently determine the nature of fluvial processes in ephemeral streams such as Yuma Wash.

Precipitation in southwestern Arizona results from a variety of atmospheric processes occurring at a number of spatial scales. The spatial extent of convective thunderstorms and orographic precipitation may be as small as only a few square kilometers, whereas frontal systems and tropical storms may extend over an area of several hundreds of square kilometers. A majority of the summer rainfall in the area of Yuma Wash is generated by isolated convective storms. Convective storms are typically limited to only a few square kilometers in extent and typically result in short duration, intense rainfall. Because of the high drainage density of sand dominated watersheds, flood-waters coalesce quickly, generating flash flooding along portions of ephemeral streams, often with little or no flow over portions of the same basin. Frontal precipitation is more common in the winter in the study area and typically provides sustained rainfall which results in more stable flows along ephemeral streams. Dissipating tropical cyclones are less common, but when they occur they have the potential of delivering tremendous amounts of precipitation over a short period of time (minutes to hours), sometimes causing extensive flooding in valley bottoms. Tropical storms are extremely variable spatially, and often result in flashy runoff over a relatively small spatial extent.

Atmospheric processes determine the sustained or flashy nature of flow in ephemeral stream systems and consequently govern fluvial processes, channel geometry, and channel features of these streams. Very different geomorphic processes occur during large, flashy runoff events than occur during longer duration, sustained flows. When examining geomorphic change on ungaged streams, it is important to consider the type of atmospheric process generating runoff in order to develop an understanding of the flow characteristics during the event.

### *Hurricane Nora*

In September 1997, tropical storms associated with Hurricane Nora entered southwestern Arizona in the vicinity of Yuma Wash. Hurricane Nora formed on September 16 over the Pacific Ocean approximately 460 km southwest of Acapulco. The tropical storm reached maximum intensity on September 21, generating wind speeds up to 213 km/hr (Rappaport 1997). Hurricane Nora entered the U.S. near the California-Arizona border on September 25 and began to dissipate. Peak wind speed recorded in Yuma, Arizona was 87 km/hr, and 2-minute sustained winds were recorded at 72 km/hr in the town of Yuma (Rappaport 1997). More than 76 cm of precipitation were recorded in parts of Arizona on September 25. This is an amount comparable to the total annual precipitation in some parts of the state.

During the storms associated with Hurricane Nora, 64% of the total annual 1997



precipitation was recorded at the remote weather stations in Yuma Wash. The largest of these storms occurred on September 5, 14, and 25 resulting in 22, 26, 31 mm of precipitation, respectively (Figure 2). The storms associated with the flooding in Yuma Wash occurred over a period of 10 hours on September 25. These storms had a maximum intensity of 9 mm/hr.

Runoff, which is determined not only by the intensity of the storm, but also the antecedent soil moisture conditions and local upland topography, generated flash flooding in many washes throughout the region, including Yuma Wash. Rainfall occurred throughout the day on September 25 following several days of smaller storms. These previous storms likely resulted in high antecedent soil moisture conditions throughout the contributing watershed of Yuma Wash. Consecutive, short duration storms often produce higher intensity flash flooding than larger isolated storms in desert streams (Leopold and Miller 1956).

Because of the high spatial variability of precipitation in the vicinity of Yuma Wash and the limited number of long-term weather stations in the area, calculations of the recurrence intervals of storms of various magnitudes are approximations. Daily total precipitation recorded at the YPG weather station located 21 km south of Yuma Wash equaled or exceeded the total precipitation recorded during Hurricane Nora 13 times over the period of record (1958 - 1997; NOAA 1998; Figure 3). The largest storm on record occurred in 1972 and was nearly three times the magnitude of Hurricane Nora. Thus these records indicate that the recurrence interval of a storm equal to the magnitude of the Nora event is approximately every 3 years. The availability of 15 minute precipitation data and pre flood cross section surveys provided a unique opportunity to document typical fluvial processes associated with natural flooding produced by a relatively frequent storm event in Yuma Wash. Yuma Wash is in turn representative of ephemeral streams throughout the lower Colorado River basin.

The objectives of this study were: (1) to use evidence of peak stage during the event to estimate peak discharge associated with Hurricane Nora, (2) to quantitatively examine the geomorphic effects of Hurricane Nora on cross sectional geometry of Yuma Wash, and (3) to determine the relative importance of valley characteristics, spatial scale (basin, reach, or cross section) of these characteristics, and hydraulic characteristics of the flood flows on the observed channel changes.

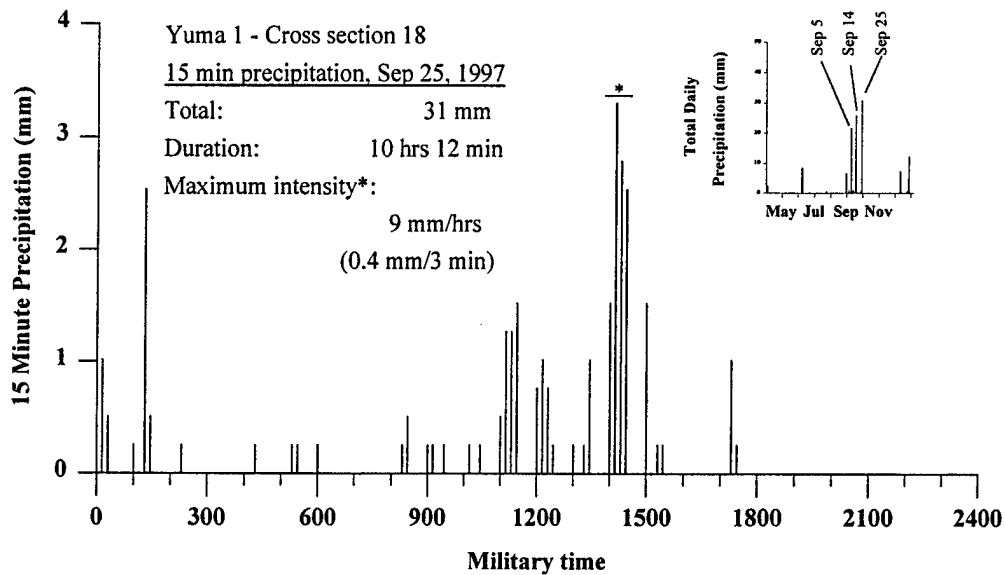


Figure 2. Daily total (inset) and 15 minute precipitation data from a remote meteorological station at cross section 18 in Yuma Wash. Maximum precipitation intensity during Hurricane Nora noted with asterisk. Unpublished data from J.D. Stednick, Colorado State University.

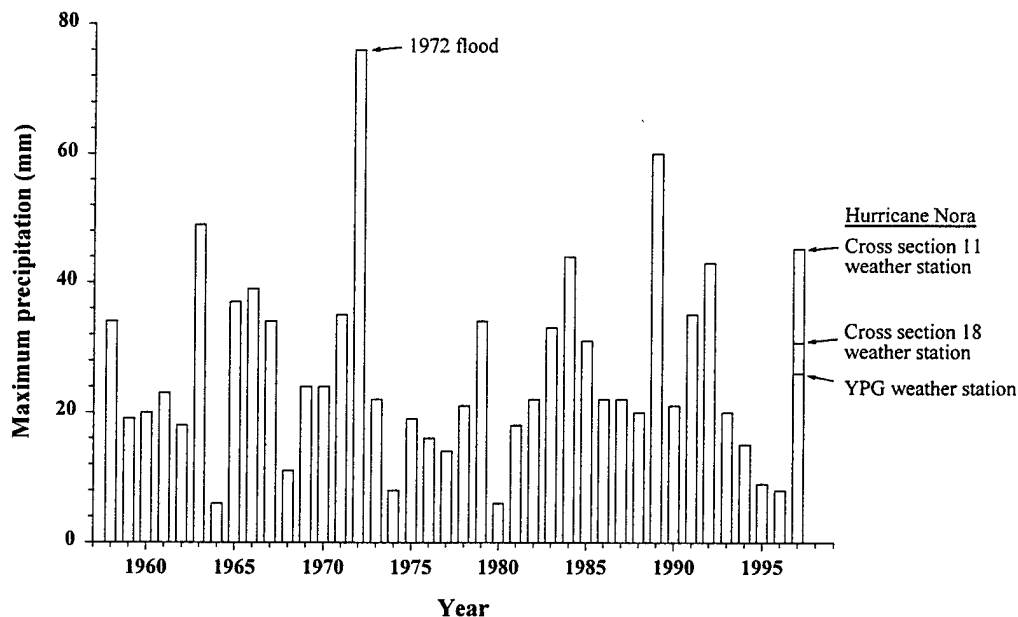


Figure 3. Historic precipitation data from the NOAA weather station at Yuma Proving Ground. The amount of precipitation on the highest rainfall day from each year showing the 1972 flood and the relative magnitude of Hurricane Nora. The three values shown in 1997 are from the NOAA station which is located 21 km south of Yuma Wash, and two remote weather stations within the wash. The remote weather stations at cross sections 11 and 18 in Yuma Wash are separated by a distance of 6 km. The differences in these values for total precipitation on September 25, 1997, illustrate the spatial variability of precipitation in the study area.

## Methods

### *Post Hurricane Nora Re-Surveys*

Field surveys were conducted in February 1997, less than six months after Hurricane Nora. It is unlikely that significant flow occurred in Yuma Wash between the initial surveys and Hurricane Nora. The largest rainfall during this period of time was 26 mm (NOAA 1998). No storm exceeded 10 mm of precipitation between Hurricane Nora and this study, therefore it is unlikely that any significant channel change occurred over this time period. Nine cross sections, which had previously been surveyed and monumented by Ayres Associates, were re-surveyed using a Topcon CTS-2 total station. Ayres Associates cross section numbers 25, 23, 21, 18, 14, 11, 4, 2, and 1 were re-surveyed as a part of this study (Figure 1). The distance from the upper cross section re-surveyed (cross section 25) to the lowest cross section re-surveyed (cross section 1) is 19.2 km. In addition, six cross sections were installed and surveyed along a stable, 100 m long bedrock-controlled reach approximately 2.0 km upstream of cross section 25, and five cross sections were installed along a 400 m reach at Ayres Associates cross section 18 (Figure 1). These additional cross sections were surveyed for the purpose of modeling flow hydraulics during the floods along these reaches. At each cross section, flood deposits were surveyed and described. Field notes were taken indicating the type and location of the deposit in relation to the channel. Flood deposits were used as indicators of water surface elevation at peak discharge during Hurricane Nora.

Flood deposits were found along channel margins or at locations where there were obstructions to flow. Flood deposits used in these analyses fell into three general categories: (1) coarse organic material, (2) fine organic material, (3) fine-grained mineral deposits (silt and fine sand). The elevation of flood deposits were surveyed in the field. During high flows, flood debris may become pushed upward against obstructions to flow a meter or more above the actual high water level in the cross section (Leopold and Miller 1956, Ayres Associates 1996). The use of such high water indicators may lead to over-estimates of stage and subsequently to over-estimates of discharge. Care was taken in selecting high water marks for peak flow estimation in this study to avoid flood deposits associated with such hydraulic ramping or deposits consisting of material trapped on rebounded plant stems. A total of 78 high water marks were surveyed throughout the wash as part of this investigation. At each of the two modeling reaches, sediment grab samples were taken from the thalweg (lowest elevation) of the main channel and maximum depth of scour was recorded. Maximum depth of scour was identified in the field by measuring the depth to a consolidated, scour resistant layer below the bed alluvium. Grab samples of bed alluvium were also taken at cross section 14 for particle size analysis. Repeat photographs were taken at each cross section for comparison with pre hurricane photographs and to aid in estimation of hydraulic roughness.

## *Hydraulic Modeling*

One-dimensional step backwater analysis and slope-area calculations using the Manning equation were the two methods used to estimate peak discharge of the flood associated with Hurricane Nora. HEC-RAS River Analysis System version 1.1 was used for step-backwater analyses (HEC 1996). Water surface slope at peak flow was used as the initial boundary condition for step backwater analyses at both modeled reaches. Energy slope was estimated by using the water surface slope at peak flow. Slope of the water surface was estimated using the elevations of high water marks at each reach. Six high water marks were surveyed along the upper modeled reach and 33 high water marks were surveyed along the cross section 18 reach.

It is acknowledged that there are many limitations to the use of one dimensional flow models for modeling flow in flashy streams with multiple flow paths. Because of the complex nature of flow in flashy systems, the use of 2-dimensional models is preferable, but requires high resolution digital elevation maps. The energy equations used in the 1-dimensional step-backwater modeling are based on the assumption of steady, uniform flow. Steady, uniform flow does not vary over time or through space, respectively. For example, in a stream under conditions of steady uniform flow, discharge does not increase or decrease over the temporal scale of consideration or as a function of distance downstream (i.e., tributary junctions). Flash flooding is by definition unsteady. Flash flood hydrographs often exhibit vertical or near vertical rising limbs, indicating instantaneous change in discharge associated with a flood wave or flood bore (Schick 1970). In order to minimize the error associated with violations of these assumptions, we selected straight reaches with relatively uniform channel geometry and lateral bedrock control, and assumed that high water marks represented a peak stage that could be modeled as steady uniform flow over a period of minutes.

To verify discharge estimates from step backwater modeling, discharge was also estimated using the Manning equation (slope-area method) for the two hydraulic model reaches. Flow was also estimated at each of the re-surveyed cross sections throughout the wash using slope-area calculations. Water surface elevation was plotted at the level indicated by high water marks at each cross section (Appendix I: Re-surveyed Cross Sections). Several hydraulic parameters (hydraulic depth, wetted perimeter, wetted cross sectional area, and water surface width) were measured from each cross section plot using the hydraulics module of the software package Scour and Fill version 7.1 (USDI 1995).

Estimated discharge from each cross section was used to develop exponential power functions to evaluate downstream hydraulic geometry of Yuma Wash (Leopold and Maddock 1953). Hydraulic geometry is the relationship between stream discharge and hydraulic characteristics of the flow (water surface width, hydraulic depth, and velocity). Hydraulic geometry relations are widely used in geomorphic investigations. Evaluating the coefficients from hydraulic geometry relations facilitates an understanding of the relationships between hydraulic variables at re-surveyed cross sections within Yuma Wash, and also enables comparisons between Yuma Wash and hydraulic relations from other ephemeral streams.

Although not measured as a part of this study, suspended sediment increases as a function of downstream distance at a more rapid rate in ephemeral streams in desert regions than in other types of streams (Schick 1970). As flow attenuates through rapid infiltration into the coarse alluvium of the bed, concentrations of suspended sediment increase. Suspended sediment is limited by supply rather than flow characteristics. This process of water loss to the bed, in combination with continual entrainment of suspended sediment, may lead to the generation of hyper-concentrated flows. In ephemeral streams, the concentration of suspended sediment increases exponentially as a function of downstream distance (Leopold and Miller 1956). General empirical relationships between the rate of increase in suspended sediment downstream and the coefficients from hydraulic geometry relations are common in the literature. These relationships will be used to estimate rates of suspended sediment increase downstream in Yuma Wash and to generate hypotheses for future studies.

Hydraulic resistance to flow involves not only grain roughness of the bed, but also energy dissipated due to bedforms, channel features, and turbulence. Roughness coefficients ( $n$ ) are the largest source of error in indirect flow estimation, particularly for large floods (Trieste and Jarrett 1987). Roughness coefficients were calculated for study reaches of Yuma Wash by taking into consideration: the grain size of the bed material, roughness related to vegetation, channel irregularities, and bedforms. The additive method developed by Cowan (1956) was used to estimate a composite  $n$  for each reach. Base values of  $n$  were estimated using the median grain size of the bed material and calculating grain roughness using an empirical equation developed by Strickler (1923). Strickler's equation is recommended for use on coarse bedded dryland streams as it was developed using data from gravel bed streams (Graf 1988). Field notes, photographs, and values calculated for other ephemeral streams in the region were all used in estimating and verifying  $n$  estimates for Yuma Wash (Arcement and Schneider 1987, Phillips et al. 1998, Phillips and Ingersoll 1998).

Discharge was estimated along the modeling reaches through an iterative process of increasing discharge and comparing calculated water surface elevations to the elevations of high water marks. Only high water marks deemed reliable markers of actual water surface level were used in discharge estimation. High water marks that appeared to have been deposited by ramping of flows onto obstructions or appeared to have been lodged into reflexed plant stems were not used to estimate discharge. Sensitivity analyses were performed by adjusting  $n$  within a range of reasonable values ( $0.03 < n < 0.06$ ) and recording discharge for each step backwater trial.

### *Calculations of Channel Change*

All survey data were registered to the Ayres Associates baseline survey using monumented cross section endpoints. All cross section elevations were converted to meters above mean sea level. Channel change was determined through comparison of pre and post hurricane channel geometry. Channel change at each cross section was quantified using four measurements: (1) area of cross sectional scour ( $m^2$ ), (2) area of cross sectional fill ( $m^2$ ), (3)

net change in channel area ( $\text{m}^2$ ), and (4) change in thalweg depth (m). Measurements of scour, fill, net change, and change in thalweg depth were calculated using the software package Scour and Fill version 7.1 (USDI 1995). The largest source of error associated with any re-survey, and ultimately with measurements of scour and fill, may be attributed to survey methodology. Small variations in the placement of survey points may result in slight miscalculations of actual scour and fill. Taking into consideration only the re-surveyed cross sections, Ayres Associates surveyed 17 points every 100 m ( $n = 384$ ) on average, whereas 32 points were measured every 100 m in this study ( $n = 684$ ) (for example see cross section 14 in Appendix 1). To reduce the inherent measurement error, scour, fill, and net channel change were taken only from portions of the cross section that were flooded during peak discharge, as indicated by recent high water marks surveyed in the field. Water level used to delineate wetted area is shown on plotted cross sections in Appendix I. Scour and fill were then normalized by dividing by channel width to obtain unit scour and fill. No transformations were applied to net change and change in thalweg depth.

When reliable water surface level indicators are available following a flood, it is possible to estimate several geomorphically important hydraulic parameters. Hydraulic variables were calculated from cross section and water surface level data for each cross section surveyed. These variables are shown in Table 1.

Table 1. Hydraulic variables measured from pre hurricane cross section geometry using the water surface elevation at peak flow during Hurricane Nora flood. Water surface elevation was estimated using high water marks at each cross section.

| Hydraulic Variable              | Units                | Equation   |
|---------------------------------|----------------------|--|
| Water surface width (W)         | m                    | $\sum(\text{water surface width of sub-channels})$   |
| Wetted perimeter (WP)           | m                    | $\sum(\text{wetted perimeter of sub-channels})$  |
| Wetted area of flow (A)         | m <sup>2</sup>       | $A = D_h W$  |
| Hydraulic depth ( $D_h$ )       | m                    | $D_h = A/W$  |
| Maximum flow depth ( $D_{mx}$ ) | m                    | --   |
| Hydraulic radius ( $R_h$ )      | no units             | $R_h = A/WP$   |
| Flow velocity (V)               | m/sec                | $V = (R_h^{0.67} s^{0.50})/n$<br>where $s$ = energy slope (approximated by water surface slope) and<br>$n$ = hydraulic roughness coefficient |
| Discharge (Q)                   | m <sup>3</sup> /s    | $Q = VA$   |
| Shear stress ( $\tau$ )         | N/m <sup>2</sup>     | $\tau = \gamma R_h s$<br>where $\gamma$ is the specific weight of water  |
| Total stream power ( $\Omega$ ) | watts/m              | $\Omega = \gamma Q s$  |
| Unit stream power ( $\omega$ )  | watts/m <sup>2</sup> | $\omega = \Omega/W$  |
| Reynold's number (Re)           | no units             | $Re = VR_h \rho / \mu$<br>where $\rho$ = density of water and<br>$\mu$ = dynamic viscosity of water  |
| Froude number (Fr)              | no units             | $Fr = V/\sqrt{(gD_h)}$<br>where $g$ = acceleration due to gravity  |

Shear stress ( $\tau$ ) is defined as the force per unit area exerted by the fluid (water) on the channel boundary (Knighton 1984). Total stream power ( $\Omega$ ) is defined as the rate of total potential energy expenditure per unit length of channel and unit stream power ( $\omega$ ) is defined as the rate of total energy expenditure per unit area of channel (Knighton 1984). In sand bed streams such as Yuma Wash, which are not sediment limited, the amount of coarse sediment that may be transported is proportional to  $\Omega$  and  $\omega$  (Inbar and Schick 1979). Reynold's number (Re) is a dimensionless variable which is derived from both the properties of water and the hydraulic properties of the channel. Re is a ratio between inertial and viscous forces in a fluid and serves as a criterion to distinguish between laminar and turbulent flow (Young et al. 1997). Froude number (Fr) is another important dimensionless hydraulic variable that describes the flow regime in an open channel. The flow regime is considered critical when  $Fr = 1$ , subcritical when  $Fr < 1$ , and supercritical when  $Fr > 1$ . Subcritical flow, also referred to as tranquil flow, typically

occurs at lower flow velocities. This flow state is preferred for hydraulics modeling because the water surface elevation is more stable for a given discharge. Using the hydraulic variables in Table 1, principal components analysis was used to calculate composite hydraulic variables. This multivariate statistical technique summarizes multiple variables into fewer composite variables which represent the structure and dimensionality of the original data. Linear regression models were then fitted by least squares to evaluate the degree to which the hydraulic variables explain the measured channel change (scour, fill, net change and change in thalweg depth).

Several physical characteristics of each cross section were measured from survey data, field notes, and 1:24,000 scale topographic maps. These variables are presented and described in Table 2.

Table 2. Physical variables measured for each cross section re-surveyed as a part of this study.

| Physical Variables                       | Units           | Description   |
|--|-----------------|---|
| Drainage basin area (Drain_A)            | km <sup>2</sup> | drainage basin area above each cross section  |
| Distance downstream (Dist)               | km              | distance downstream from cross section 25   |
| Valley width (Val_w)                     | m               | valley width at the cross section   |
| Rate of change in valley width (Rate_vw) | m/m             | the rate of change in valley width upstream from the cross section; calculated by dividing the difference in valley width 200 m above the cross section and at the cross section, by 200 m.             |
| Bedrock                                  | --              | binary variable: value of 1 if bedrock confinement was noted on at least one side of the channel at the cross section, and 0 if bedrock was not present through the 200 m reach above the cross section |
| Valley slope (slope)                     | m/m             | bedslope through the reach 200 meters upstream and downstream of the cross section (m/m)  |
| Number of channels (No_chan)             | --              | number of channels and subchannels at a cross section   |
| Percent vegetation (Perc_veg)            | %               | percent of the cross section width vegetated estimated from oblique photographs   |

Stepwise regression was used to determine which of the variables presented in Table 2 best explained the net change in cross section dimensions caused by the Hurricane Nora flood.

Cross sections were classified into one of two categories (aggraded or degraded) based on net change in channel geometry from pre to post hurricane surveys. Stepwise discriminant analysis was used to develop a function to categorize cross sections as aggraded or degraded based on the physical attributes of the channel. Stepwise analysis was also performed on hydraulic variables. Statistical difficulties may be encountered when a large number of



independent variables are used relative to the number of samples. Because of the limited number of cross sections used in the analysis ( $n = 9$ ), the final discriminant function was limited to only the two most significant variables in the stepwise analysis. These classification analyses provide not only information concerning what variables best describe whether a particular cross section is likely to aggrade or degrade, but the discriminant function also provides a means of categorizing cross sections for which re-surveys were not conducted. This predictive use of the discriminant function is valid only after the function is shown to do an adequate job of correctly classifying the cross sections that were re-surveyed.

### *Spatial Scale Controls on Channel Change*

Channel morphology at any point in time is the product of some balance between driving and resisting forces, and the amount of sediment available to the channel. The flow of water is the primary driving force in ephemeral streams, and is determined largely by the amount of water delivered to the channel from the surrounding landscape and upstream and channel slope. Abrasive material transported by the flow (mineral and woody debris) may also serve as scouring agents. The amount of flow in an ephemeral stream is a function of the drainage basin area, size and intensity of the precipitation, and permeability and relief of the ground surface. Landscape features that provide resistance to scouring and entrainment of bed materials include: stems and roots of vegetation in the channel, packing, armoring, or chemical cementation of bed materials, and the composition (size and orientation) of alluvial substrates. These factors are characteristics acting at the scale of individual cross sections. Valley shape and the change in valley width as a function of distance downstream are reach scale factors. Physical attributes of the valley influence sediment processes and channel morphology by governing flow contraction and expansion, which influences the distribution of energy exerted by the flow on the channel boundary. In summary, each of these factors influence the ability of the flow to modify channel geometry through entraining and transporting sediment, and each of these factors are controlled at different spatial scales.

The physical attributes of Yuma Wash described in the previous section were categorized into one of three spatial scales for further analysis. Each of the measured variables was placed into either basin scale, reach scale, or cross section scale categories (Table 3). Basin scale attributes include drainage basin area above each cross section and distance downstream. Reach scale attributes include the rate of change in valley width above each cross section, the presence or absence of bedrock, and valley slope through the reach. Cross section scale attributes include the percent of the cross section vegetated, the valley width at the cross section, and the number of channels and subchannels at the cross section.

Principal components analysis was used to summarize the data at each spatial scale into fewer, representative composite variables. These composite variables were then used to explain the measured change in channel dimensions at the re-surveyed cross sections. Separate multiple linear regression analyses were conducted at each spatial scale to determine whether basin, reach, or cross section scale attributes best explain channel change. The relative importance of

basin scale versus reach or cross section scale controls on channel change, could provide valuable information concerning the likely effects of land-uses at different spatial scales on channel form within Yuma Wash. It was hypothesized that all three scales would influence channel form, but to different degrees.

Table 3. Spatial scale of physical variables measured for each cross section re-surveyed as a part of this study. Refer to Table 2 for descriptions of each of the physical variables.

| Spatial Scale Category | Physical Variables             |
|------------------------|--------------------------------|
| Basin scale            | Drainage basin area            |
|                        | Distance downstream            |
| Reach scale            | Rate of change in valley width |
|                        | Bedrock                        |
|                        | Valley slope                   |
| Cross section scale    | Valley width                   |
|                        | Number of channels             |
|                        | Percent vegetation             |

#### *Classification of Cross Sections Based on Physical Attributes*

As a part of the descriptive baseline study of Yuma Wash, Ayres Associates categorized the wash into four reaches based upon physical characteristics of the valley and number of channels at the surveyed cross sections (Ayres Associates 1996). These classifications were largely subjective, but gave a useful overall characterization of the variability in valley attributes throughout the wash. In an attempt to verify this classification and to develop an understanding of how channel response to flash flooding differs along different valley segments, we used several independent physical attributes of each cross section to classify each cross section into one of four groups. Average linkage cluster analysis was used for this classification. This type of cluster analysis is an agglomerative method, which groups like objects based on similarities in their physical attributes. In this application, the objects are cross sections. Attributes used to cluster cross sections were: (1) valley slope, (2) valley width, (3) rate of change in valley width, (4) presence of bedrock one or both sides of the cross section, (5) number of channels or subchannels, and (6) percent vegetation cover. We then compared this objective grouping to the placement of cross sections into each of the four geomorphic categories developed by Ayres Associates. We also provide mean values of cross section and hydraulic attributes of each cluster and a description of each objectively classified reach type.

## Results and Discussion

### *Hydraulics Modeling and Slope-Area Flow Estimates*

Water surface slope was 0.007 for the upper modeled reach and 0.010 for the cross section 18 reach. Water surface slope corresponded well with surveyed bedslopes, which were 0.006 and 0.010, respectively (Table 4). These relatively steep slopes are typical of braided streams.

After plotting the high water marks and reviewing the field notes, it became apparent that there were two distinct sets of high water marks throughout the wash. A group of very old, high water marks deposited above the more recent deposits associated with Hurricane Nora, provided evidence of a significantly larger flood which had occurred historically. These historic high water marks had been deposited at heights of 20 cm to 105 cm above those deposited by Hurricane Nora. Flows of this historic event were estimated for comparison with the Hurricane Nora flood using step backwater modeling and the slope-area method. The slope-area method was used to estimate peak discharge of this historic flood for all other re-surveyed cross sections as well. Roughness values were held constant.

It was impractical to precisely date these deposits, but field notes indicated that they were comprised of 'very old' woody debris. Historic precipitation data from weather station at YPG indicate that the three largest storms on record occurred in 1963, 1972, and 1989 (NOAA 1997) (Figure 3). The largest of these storms (76 mm) occurred on October 6, 1972. The second and third largest precipitation days on record had magnitudes of 60 mm on August 9, 1989 and 49 mm on September 17, 1963. The 1963 storm was an isolated event, occurring 13 days after the previous precipitation. Less than one mm of precipitation was recorded the day before the 1983 storm. Precipitation was recorded two of the three days before the 1972 storm, during which time one mm of precipitation was measured at YPG (NOAA 1997). Considering the relative magnitude, precipitation on previous days, and age of the flood deposits, we conclude that the historic high water marks modeled in this study were likely deposited during flooding associated with a frontal storm system on October 6, 1972.

Base roughness coefficients were calculated from bed grain size distributions (Appendix III). The roughness coefficient was estimated to be  $n = 0.018$  for the upper modeled reach and  $n = 0.020$  for Ayres cross section 18. Adding energy losses due to cross section shape, channel variation, obstructions to flow, vegetation, and sinuosity, increased these base values to  $n = 0.051$  for the upper modeled reach and  $n = 0.046$  for cross section 18. Ayres Associates (1996) applied a general roughness coefficient of  $n = 0.035$  to all cross sections in Yuma Wash for rainfall runoff modeling. Peak flow of the Hurricane Nora flood was estimated using the Ayres Associates  $n$  value as a low estimate, hydraulic roughness values estimated through the additive method in this study, and higher estimates than are likely, to include a full range of possible discharges. Hydraulic roughness values of  $n = 0.045$  were used for all slope-area discharge estimates at all re-surveyed cross sections in this study. Phillips et al. (1998) and Phillips and

Ingersoll (1998) conducted studies of roughness in natural and constructed stream channels throughout Arizona. Many of the streams in these studies exhibit characteristics similar to Yuma Wash. House (1997) selected a roughness coefficient of  $n = 0.040$  for flow modeling of probable maximum floods for ephemeral streams throughout southwestern Arizona. Roughness estimates for Yuma Wash correspond well with those in similar ephemeral systems represented in these studies.

Table 4. Bedslope, water surface slope estimated from high water marks, roughness coefficients used in step backwater analyses, and estimated discharges associated with Hurricane Nora. Italics indicate discharge estimates using higher and lower roughness coefficients than the preferred value which was estimated using the additive method. Final maximum flow estimates are in bold type.

| Reach       | Bedslope | Water surface Slope | Base Roughness Coefficient | Roughness Coefficient | Discharge m <sup>3</sup> /s |
|-------------|----------|---------------------|----------------------------|-----------------------|-----------------------------|
| Upper XS    | 0.006    | 0.007               | 0.018                      | 0.035                 | 35                          |
|             | 0.006    | 0.007               | 0.018                      | 0.051                 | <b>21</b>                   |
|             | 0.006    | 0.007               | 0.018                      | 0.060                 | <i>18</i>                   |
| Ayres XS 18 | 0.010    | 0.010               | 0.020                      | 0.035                 | <i>48</i>                   |
|             | 0.010    | 0.010               | 0.020                      | 0.046                 | <b>39</b>                   |
|             | 0.010    | 0.010               | 0.020                      | 0.050                 | <i>34</i>                   |

Using these values of water surface slope and additive roughness coefficients (Table 4) in step backwater analysis, peak flow estimates were 21 m<sup>3</sup>/s through the upper reach and 39 m<sup>3</sup>/s at cross section 18. These discharge estimates were those that generated the best visually fit water surface through the high water marks (Figures 4 and 5). Adjusting roughness coefficients down to the roughness coefficient estimated by Ayres Associates ( $n = 0.035$ ) resulted in increases in peak discharge estimates to 35 m<sup>3</sup>/s and 48 m<sup>3</sup>/s for the two modeled reaches, respectively. Final peak discharge estimates for the Hurricane Nora floods were 21 m<sup>3</sup>/s and 39 m<sup>3</sup>/s for the upper reach and cross section 18, respectively.

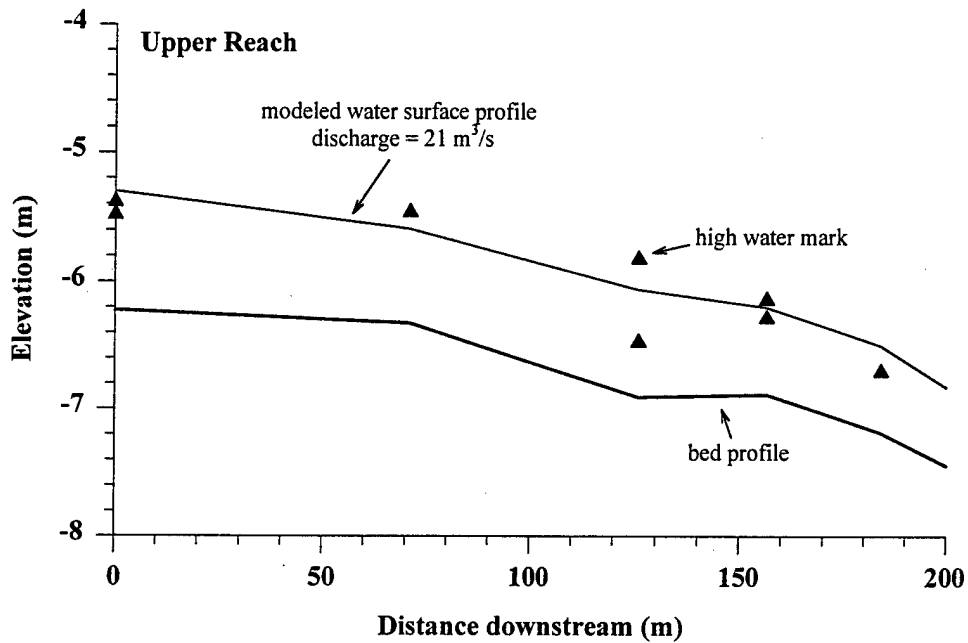


Figure 4. Modeled water surface profile at a discharge of  $21 \text{ m}^3/\text{s}$ . Flow was estimated from high water marks deposited during Hurricane Nora.

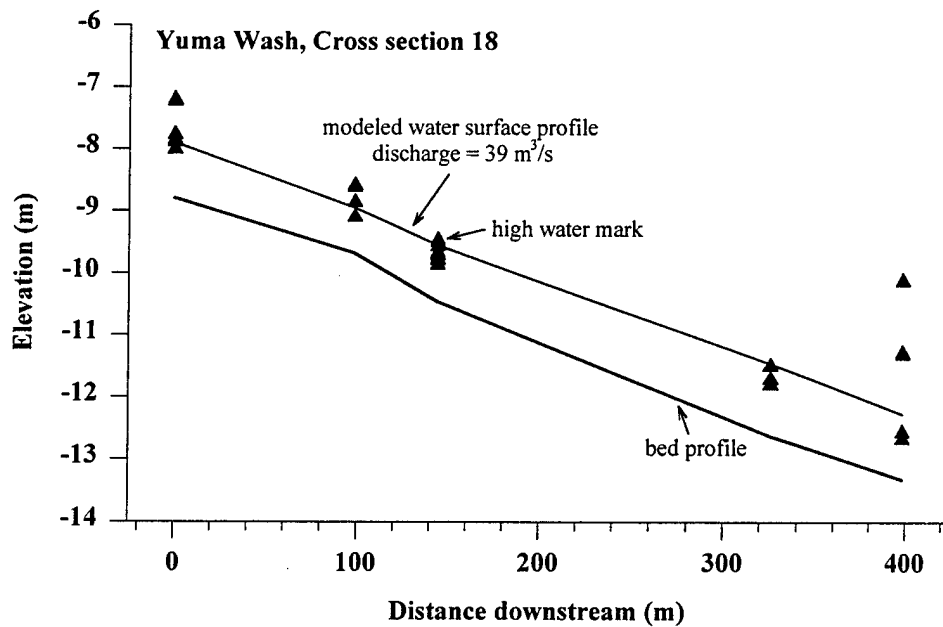


Figure 5. Modeled water surface profile at a discharge of  $39 \text{ m}^3/\text{s}$ . Flow was estimated from high water marks deposited during Hurricane Nora. High water marks from the historic flood are evident.

Slope-area estimates of discharge during Hurricane Nora compared well with estimates using step-backwater methods. Discharge at cross section 18 was estimated to be 44 m<sup>3</sup>/s. Throughout the wash, peak flow during Hurricane Nora ranged from a low of 16 m<sup>3</sup>/s at cross section 21 to a high of 237 m<sup>3</sup>/s at cross section 1 (Figure 6). Turbulent flow was well developed throughout the wash during the flood. Reynold's numbers ranged from 2.47e<sup>5</sup> to 1.04e<sup>6</sup>. Flow was subcritical at peak discharge at all cross sections. Froude numbers ranged from a low of 0.62 at cross section 21 to a high of 0.92 at cross section 25.

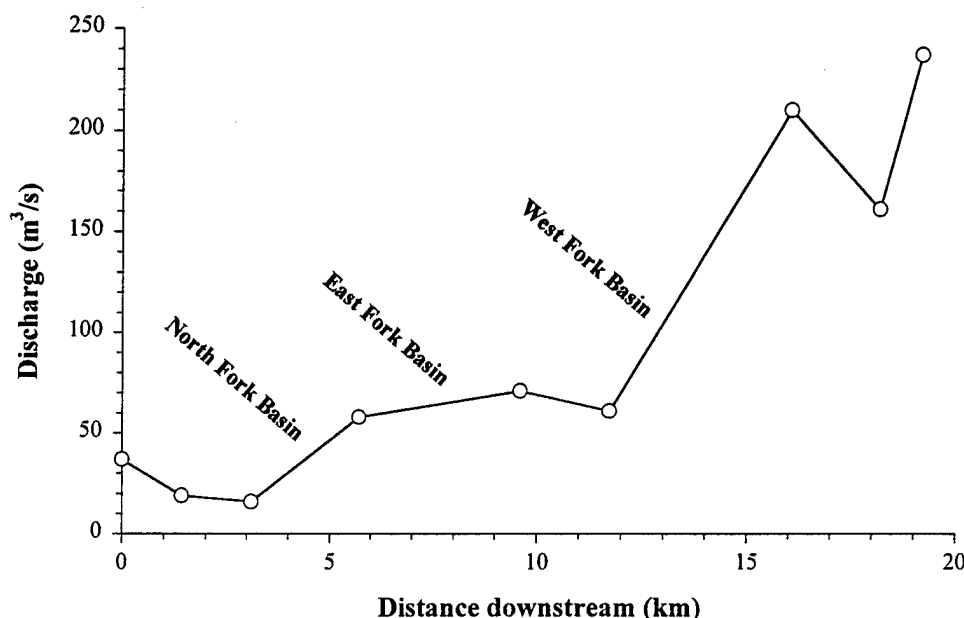


Figure 6. Discharge as function of distance downstream during Hurricane Nora flood. Cross section 25 is the furthest upstream (distance = 0 km) and cross section 1 is the furthest downstream (distance = 19.2 km). Approximate locations of confluences with sub-basins of the wash are indicated.

Estimated discharge to obtain a modeled water surface elevation of historic high water marks deposited during the historic 1972 flood, was 210 m<sup>3</sup>/s at cross section 18. Stage indicators at the upper modeling reach were not considered reliable for this historic-flow event, therefore flow was not modeled through this reach. However, reliable high water marks were surveyed at all re-surveyed cross sections and flow was estimated at each of these. Flow was supercritical at all cross sections during peak discharge of the historic flood. Reynolds numbers ranged from 5.28e<sup>5</sup> to 6.07e<sup>6</sup>, indicating that turbulent flow was very well developed at all cross sections during the flood. Discharge increased nearly six fold in a downstream direction, increasing from 193 to 1280 m<sup>3</sup>/s. The maximum peak discharge during this historic flood was 1280 m<sup>3</sup>/s, a value which falls neatly within the regional envelope curve of maximum peak discharges calculated for ephemeral streams throughout the lower Colorado River Basin for drainage areas the size of Yuma Wash (186 km<sup>2</sup>; House 1997). Thus, this discharge estimate provides a reasonable magnitude for the probable maximum flood in Yuma Wash.

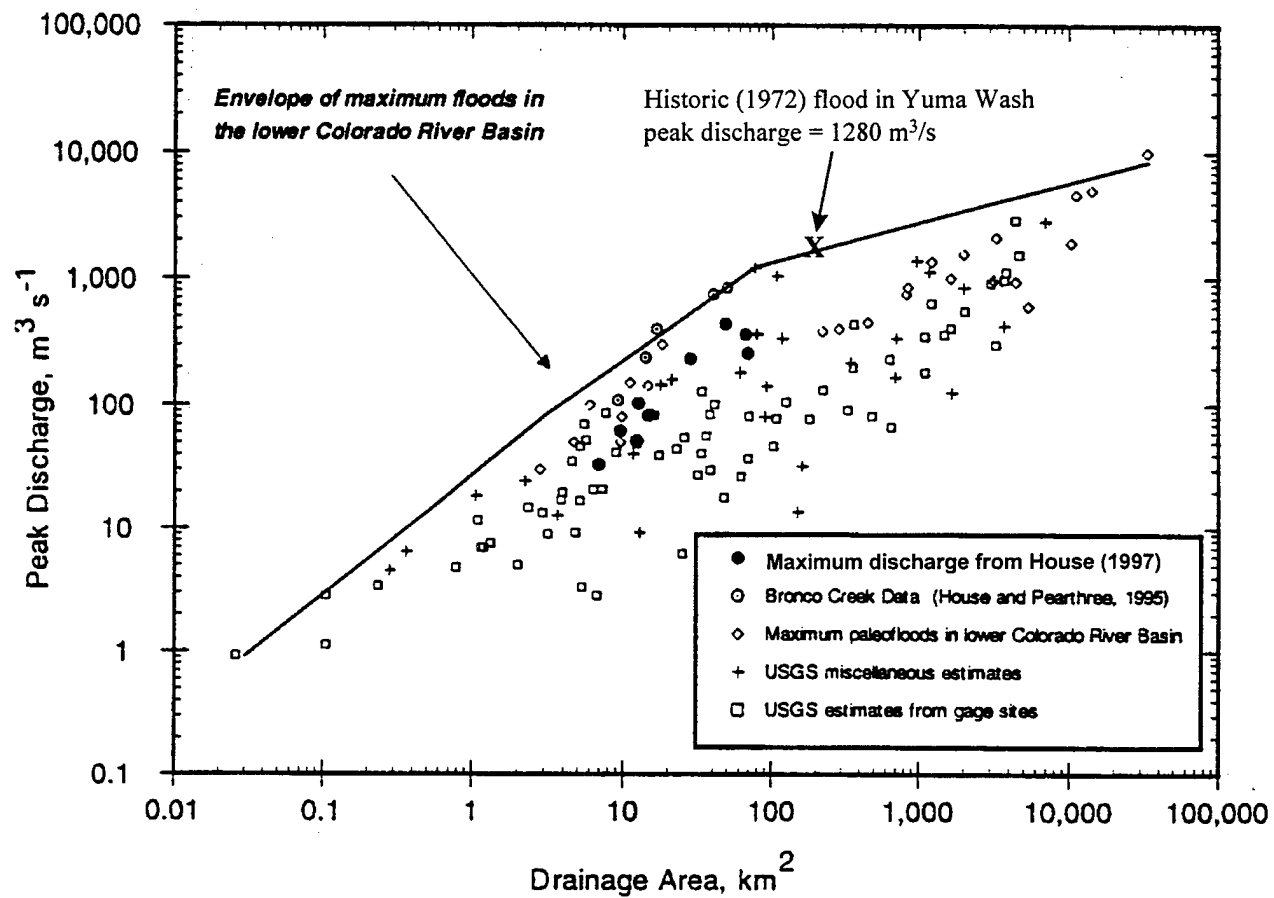


Figure 7. Comparison of the maximum peak discharge for a historic flood in Yuma Wash to the regional envelope curve of maximum peak discharges versus drainage area in the lower Colorado River Basin (from House 1977).

Investigations on other ephemeral streams throughout the southwestern United States, in catchments ranging from 0.6 km<sup>2</sup> to 4200 km<sup>2</sup>, indicate that flow increases in a downstream direction at a faster rate on ephemeral streams than on perennial streams with similar sized catchments (Leopold and Miller 1956). Ephemeral streams in arid regions tend to increase in width at a lower rate as a function of discharge, and increase in velocity as a function of discharge at a higher rate in a downstream direction than perennial streams and ephemeral streams in humid regions (Cooke et al. 1993). Yuma Wash downstream hydraulic geometry relations are presented in Figure 8. Table 5 provides hydraulic geometry coefficients calculated as a part of this study as well as coefficients from ephemeral streams in other arid and semi-arid regions throughout the world.

Table 5. Hydraulic geometry relations for ephemeral streams in Europe and central and southwestern North America (Cooke et al. 1993). Coefficients for Yuma Wash are from this study. The rate of change in width as a function of discharge ( $b$ ), rate of change in depth as a function of discharge ( $f$ ), and rate of change in velocity as a function of discharge ( $m$ ) are indicated. The rate of change in suspended sediment concentration as a function of discharge ( $j$ ) is estimated by the equation  $m/f$  in all cases except the New Mexico study, where it was measured (Leopold and Miller 1956).

|                        | Humid Region |            | Arid regions    |           |
|------------------------|--------------|------------|-----------------|-----------|
| Downstream coefficient | Nebraska     | New Mexico | Southeast Spain | Yuma Wash |
| $b$                    | 0.03         | 0.50       | 0.63            | 0.78      |
| $f$                    | 0.48         | 0.30       | 0.20            | 0.15      |
| $m$                    | 0.45         | 0.20       | 0.17            | 0.14      |
| $j$                    | 0.94         | 1.3        | 0.85            | 0.93      |

Water surface width of Yuma Wash increased with discharge at a more rapid rate than any of the other ephemeral streams in Table 5. One explanation for the exponential rate of widening with increasing discharge downstream is the composition of the bed and bank material. Width/depth ratios are typically higher on streams that have low levels of silt and clay in their bed and bank material (Schumm 1960). Particle size distributions indicate that silt and clay comprise less than 3% of the bed material in Yuma Wash (Appendix III). Width/depth ratios in Yuma Wash ranged from 60 to 387. Median grain size ( $D_{50}$ ) in the upper reaches of the wash was 3 mm, 4 mm at cross section 18, and 2 mm at cross section 14.



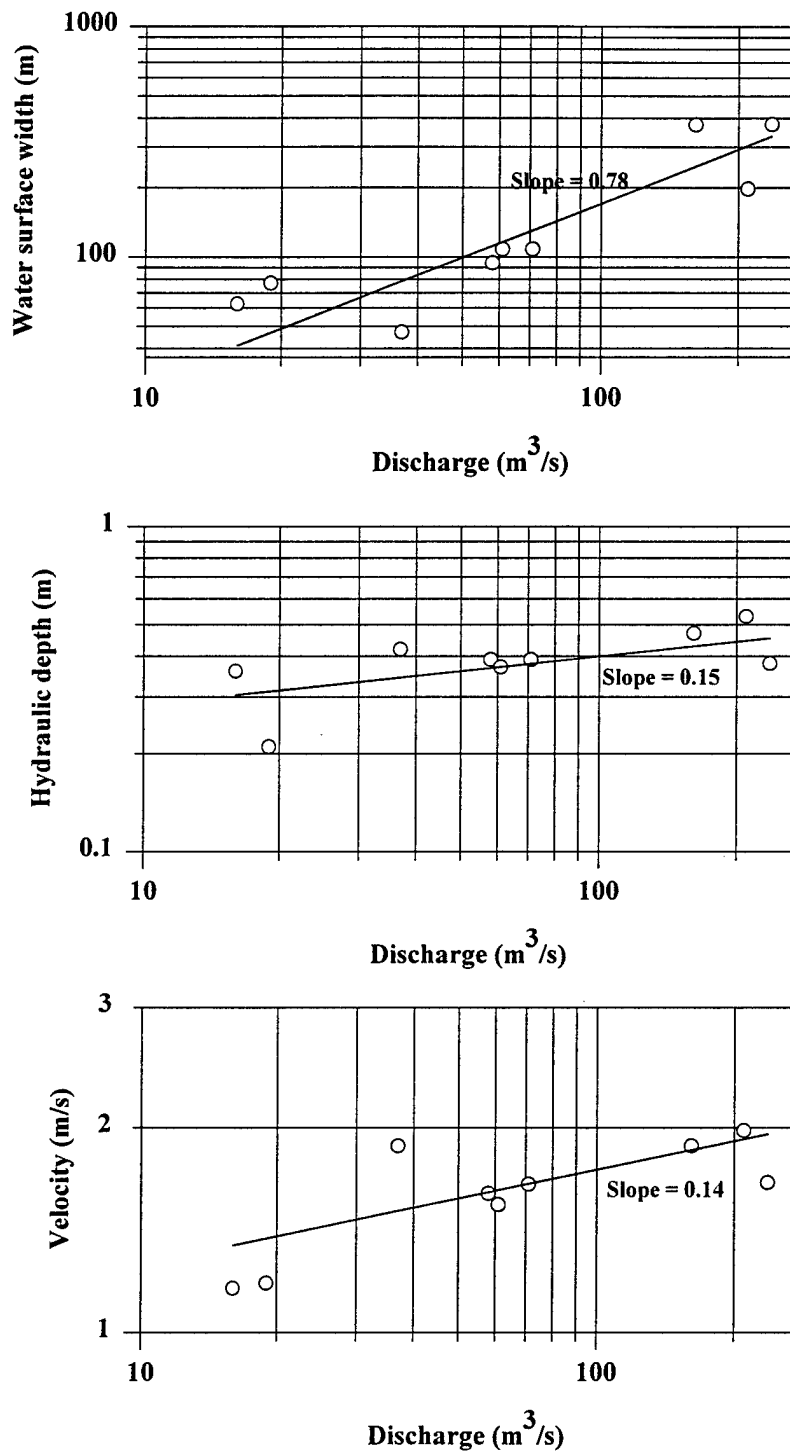


Figure 8. Downstream hydraulic geometry relations in Yuma Wash during Hurricane Nora flood. See Table 5 for hydraulic geometry relations from other streams.

## *Channel Change*

Significant channel change occurred along some reaches of Yuma Wash as a consequence of flooding associated with Hurricane Nora (Figure 9, Appendix I). Six of the nine re-surveyed cross sections experienced net bed aggradation (net fill) during these flows and three cross sections experienced net degradation (net scour). Average net change of aggrading cross sections was  $12.1 \text{ m}^2$  (standard error =  $\pm 4.5 \text{ m}^2$ ), whereas the average net change of scoured channels was  $-5.8 \text{ m}^2$  (se =  $\pm 2.3 \text{ m}^2$ ). Average thalweg change was consistent with this trend; increase in thalweg elevation occurred at cross sections that aggraded, and the thalweg typically scoured at cross sections that experienced net scour. Average change in thalweg depth was 5 cm ( $\pm 9$  cm) at cross sections that aggraded, and -14 cm ( $\pm 2$  cm) at cross sections that scoured. In general, net aggradation and thalweg accretion occurred along wider valley reaches and where channels and subchannels were more numerous, and net scour and thalweg scour were greater where the valley was narrower and flow was confined to fewer channels. Locally, fill occurred upstream and downstream from obstructions to flow. Fill of 11 to 22 cm occurred around military target cars in the channel during Hurricane Nora (Appendix II, Plate 5).

Net fill was considerably higher in cross sections furthest downstream in the wash. Net scour was greatest at intermediate distances downstream. Over the length of the wash re-surveyed, degrading reaches alternated with aggrading reaches (Figure 9). Cross section 25 exhibited little change as a consequence of hurricane flows. Cross section 23 scoured. Cross sections 21 and 18 aggraded. Cross sections 14 and 11 scoured. Cross section 4, 2, and 1 aggraded significantly. Patterns of aggradation and degradation suggest a wavelike movement of sediment through the 19.2 km reach surveyed. These patterns could be attributed to an event-driven, pulsed movement of sediment through the wash. Long-term (20 year) re-survey data from an alluvial stream in northern California indicated that aggradation and degradation were related to a sediment wave propagating downstream through time (Madej and Ozaki 1996). Cross sections were shown to aggrade or degrade at different points in time depending on their position in relation to this wave of sediment. Such a process could obscure direct relationships between physical attributes of cross sections and their likelihood of aggrading or degrading over the course of a single flood. Alternatively, the wavelike patterns measured in Yuma Wash may have been influenced by the balance between water and sediment discharge from tributary inflows from the sub-basins of the wash.

The magnitude and intensity of contributing flows from each of the sub-basins of the wash to the mainstem of Yuma Wash is a function of the intensity and spatial variability of the rain event, the size of the sub-basin receiving precipitation, the rate of runoff from the land surface, and the hydraulic properties of the valley bottom in the sub-basin. As was previously mentioned, three sub-basins or tributaries enter the main-stem of Yuma Wash through its length: the North Fork Basin enters the wash below cross section 21, the East Fork Basin enters the wash below cross section 18, and the West Fork Basin enters the wash below cross section 11. Discharge estimates from the re-surveyed cross sections indicate that the North Fork Basin contributed  $41 \text{ m}^3/\text{s}$  to the main-stem Yuma Wash at peak flow (Figure 6). The East Fork Basin

contributed about 12 m<sup>3</sup>/s. The West Fork Basin contributed 149 m<sup>3</sup>/s to the main-stem Yuma Wash at peak flow. In this case, the variability in the contribution of flow from the sub-basins to

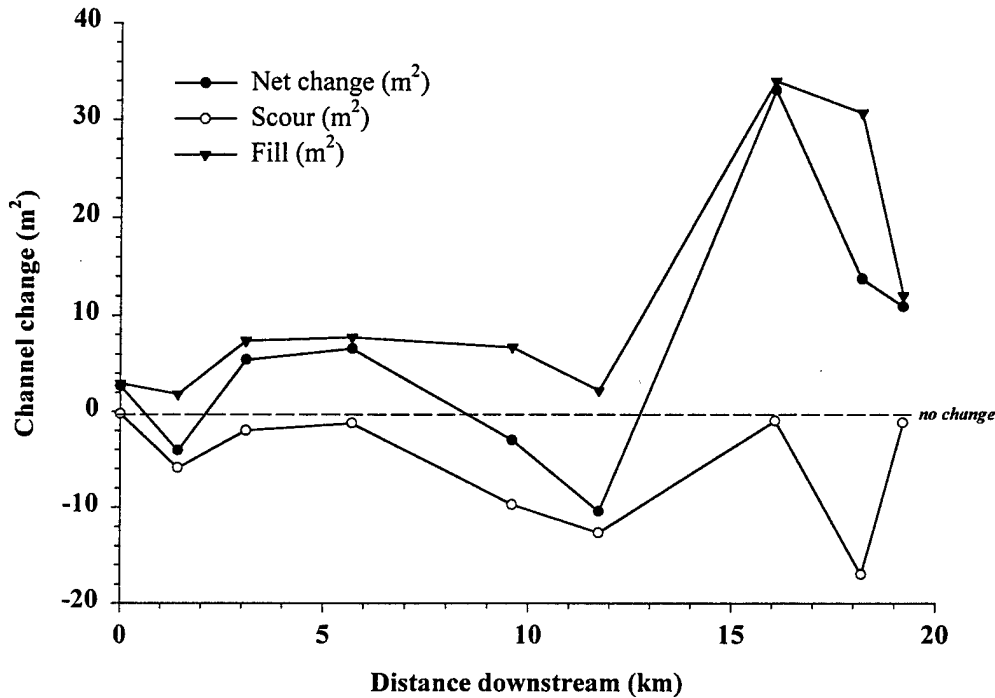


Figure 9. Changes in channel geometry of Yuma Wash from cross sectional surveys measured prior to and following flooding associated with Hurricane Nora. Cross section 25 is the furthest upstream (distance = 0 km) and cross section 1 is the furthest downstream (distance = 19.2 km).

the main-stem of Yuma Wash is a function of the spatial variability in the intensity of precipitation during the hurricane rather than a function of the differences in the watershed areas of the sub-basins of the wash. Variations in sediment supply, caused by differential rates of erosion within the sub-basins of the wash, may provide an explanation for the downstream variations in scour and fill in the wash over both the short and long-time scales. Using cosmogenic isotopes to estimate erosion rates in Yuma Wash, Clapp and Bierman (1998) found that erosion rates of sub-basins of Yuma Wash may be different than average erosion of all the sub-basins.

The watershed areas of each of the basins is similar, ranging from 34 - 43 km<sup>2</sup>. Flow contributions of each of the sub-basins indicate that the storm was centered over the West Fork Basin. This assertion is further supported by the meteorological station 15 minute precipitation

data from the day of the hurricane. The total precipitation measured on September 25 was 31 mm and 13 mm at cross section 18 and cross section 11, respectively. The highest precipitation intensity was 4.9 mm/hr and 0.7 mm/hr at cross sections 18 and 11, respectively. Cross section 18 is located nearest the North Fork Basin and cross section 11 is in close proximity to the West Fork Basin (Figure 1). Net fill occurred in the reach below the confluence with the North Fork, net scour occurred below the confluence with the East Fork, and net fill occurred below the confluence with the West Fork. It is hypothesized from these patterns that discharge must be above some threshold for substantial net fill to occur. Perhaps discharge must be of sufficient volume to overtop in-channel bars which separate individual split-flow paths. At lower discharges, flow is confined to deep, unvegetated, swifter flowing channels and net scour results. At higher discharges, stage is sufficient to overtop vegetated bars. Flow velocity decreases over bars, in part because of higher roughness, which facilitates sediment deposition. Secondary flow cells in channels between bars may facilitate scouring and maintenance of unvegetated channels between vegetated islands, as proposed by Wende and Nanson (1998). These secondary flow cells, which scour sediment from channels and deposit sediment on bars, may produce regularly spaced bar and channel sequences in braided streams such as Yuma Wash. Linear bands of vegetation oriented downstream, were evident at many of the re-surveyed cross sections in Yuma Wash (see Plates 2, 6 and 8 in Appendix II).

Multiple regression model selection using physical attributes of the wash rather than hydraulics of the hurricane Nora flood, indicates that the number of channels at a particular cross section is the most important physical channel characteristic in determining the degree and direction of channel change. Regression models using these physical attributes rather than hydraulic variables, explain little of the variability in cross sectional change ( $r^2 = 0.36$ ,  $p = 0.09$ ). In contrast, the hydraulic attributes of the cross sections at high flow during Hurricane Nora were significant predictors of thalweg scour, net change, and fill (Figures 10 and 11, Table 6).

Table 6. Regression models constructed using stepwise model selection of hydraulic variables from each cross section. Model parameters, regression coefficients, and model p-values are provided. N/S indicates that no hydraulic variable met the  $p = 0.15$  significance level for inclusion into the model. Hydraulic variables were calculated from high water marks at each cross section. Variables included in the model selection routine were: water surface width (m), wetted perimeter (m), wetted area of flow ( $m^2$ ), hydraulic/average flow depth (m), maximum flow depth (m), velocity (m/s), discharge ( $m^3/s$ ), shear stress ( $N/m^2$ ), total stream power (watt/m), and unit stream power (watts/ $m^2$ ). Maximum depth and average depth were the only significant hydraulic variables.

| Model Parameters   | Diagnostics                |
|--|----------------------------|
| Thalweg change (m) = $-0.77 + 0.81 * (\text{Maximum depth})$   | $r^2 = 0.41$ , $p = 0.060$ |
| Net change ( $m^2$ ) = $-59.2 + 70.4 * (\text{Maximum depth})$ | $r^2 = 0.72$ , $p = 0.004$ |
| Unit Scour (m) = NS  | --                         |
| Unit Fill (m) = $-0.13 + 0.52 * (\text{Hydraulic depth})$      | $r^2 = 0.63$ , $p = 0.010$ |

Stepwise discriminant analysis of cross section attributes resulted in the selection of two

variables: valley width and number of channels and subchannels. These two variables best classify cross sections as aggrading or degrading. The discriminant function containing these two variables which characterize the cross section, correctly categorized 67% of re-surveyed cross sections as aggraded or degraded. The discriminant function mis-classified cross sections 18 and 25 as degraded whereas they actually aggraded  $6.6 \text{ m}^2$  and  $2.7 \text{ m}^2$ , respectively. Cross section 11 was misclassified as aggraded when it actually degraded by  $10.4 \text{ m}^2$ .

In general, the discriminant function based on cross section attributes classified cross sections with wider valleys and numerous multiple channels as aggraded. Cross sections in narrower valleys with fewer channels were classified as degraded.

Stepwise discriminant function analysis using hydraulic characteristics of the flows associated with Hurricane Nora resulted in a very robust discriminant function. One variable, maximum depth of flow, was selected over all other variables for the final discriminant function. The function containing maximum depth of flow correctly classified eight of the nine re-surveyed cross sections (89%). Cross section 25 was incorrectly classified as degraded. Given water surface elevations from the 13 cross sections that were not re-surveyed as a part of this study, this discriminant function could be used to classify these cross sections as aggraded or degraded with an estimated accuracy of 89%. In general, this discriminant analysis indicates that cross sections with greater maximum flow depth aggrade, whereas those with lower flow depths degrade. Flow depth is a function of cross sectional geometry, discharge, and boundary roughness. During Hurricane Nora, flow depth increased with distance downstream at an exponential rate of 0.15 (Table 5, Figure 8).

As previously mentioned, higher flow volumes facilitate the flooding of bars and inter-channel features. These depositional features are located in areas of energy dissipation. In these areas, shear stress is lower than within deeper portions of the channel and vegetation may become established. The presence of vegetation and the shallower flow depths over these features increase the hydraulic roughness of the surface. The decrease in flow velocity caused by increased hydraulic roughness from plant stems may substantially decrease the sediment transport capacity of the flow, even during relatively high flows. At lower discharges when flow is confined to multiple channels, inter-channel bar growth can not occur through vertical accretion. Therefore high flows are necessary for substantial net aggradation of cross sections to occur.

Given a water surface level related to some discharge at a particular cross section, the width of the valley, and the number of channels conducting flow, the discriminant function has an acceptable ability to predict whether the cross section will aggrade or degrade. The quantity of net scour or fill was also found to be a function of maximum depth of flow. In regression analyses, maximum depth of flow explains 72% of the variability of scour or fill measured in Yuma Wash ( $r^2 = 0.72$ ;  $p = 0.004$ )(Table 6). Discharge was greatest at the lowest three cross sections in the wash (cross sections 4, 2, and 1) and depth of flow was greatest at these cross sections as well.

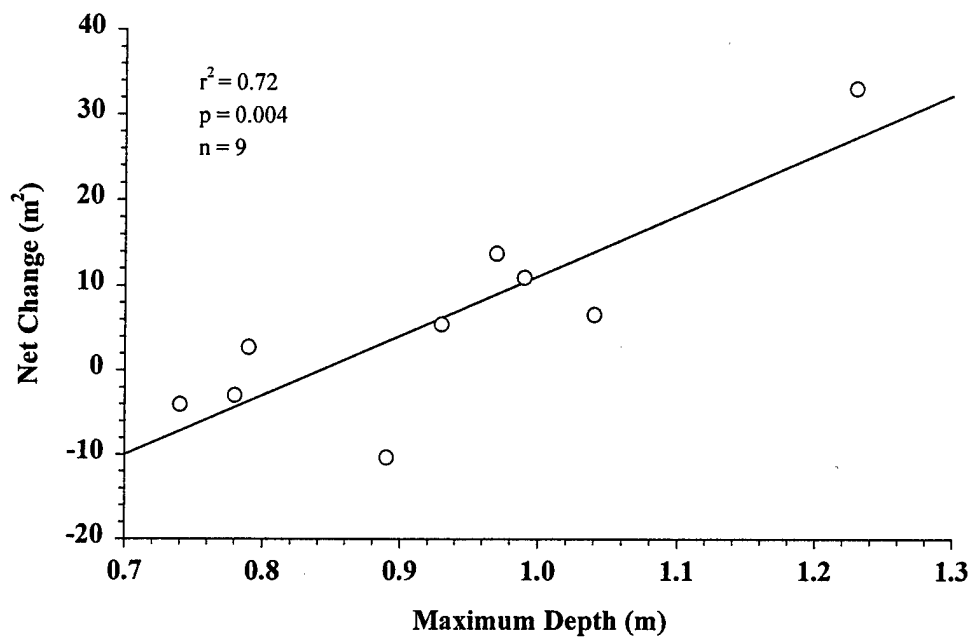


Figure 10. Net channel change plotted as a function of maximum depth of flow. Regression coefficients presented in Table 3.

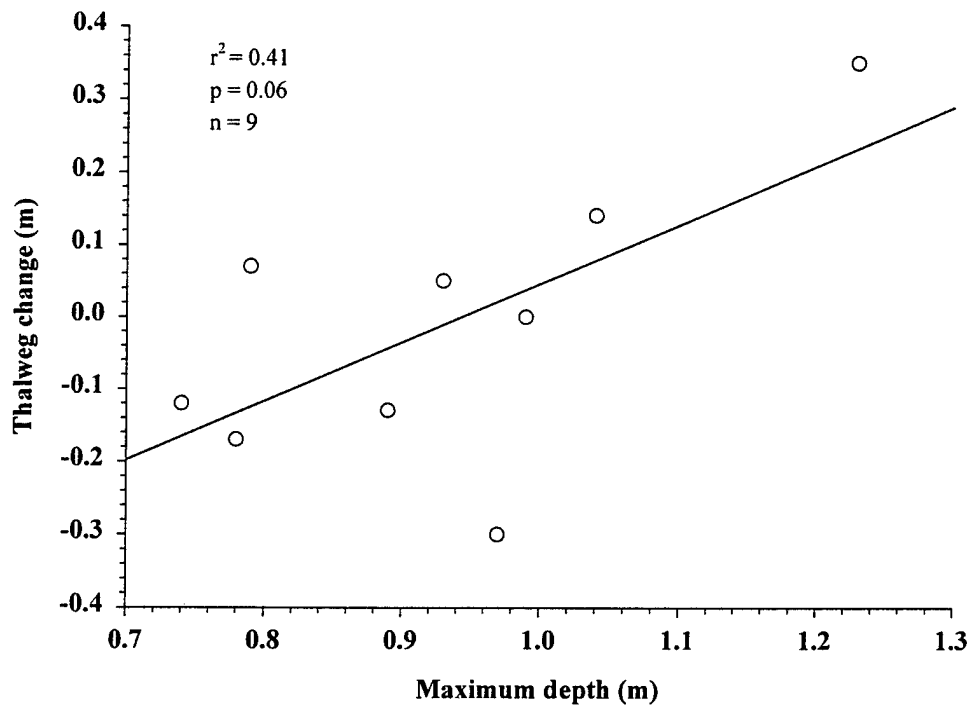


Figure 11. Thalweg change plotted as a function of maximum depth of flow. Regression coefficients presented in Table 3. The outlier, at -0.3 m thalweg change, is cross section 2.

### *Spatial Scale Controls on Channel Change*

Cross-section scale principal components did not significantly explain measured channel changes. The strongest relationship between cross-section scale principal components and channel change was between the first two principal component axes and unit fill of the channel. This relationship was not statistically significant ( $r^2 = 0.25$ ,  $p = 0.41$ ). Channel fill was greatest in wider valleys with multiple channels and where percent cover of vegetation was lower. Reach-scale principal components produced the most significant models in this spatial scale analysis. Reach-scale attributes were significant predictors of thalweg change ( $r^2 = 0.71$ ,  $p = 0.02$ ) and unit scour ( $r^2 = 0.92$ ,  $p = 0.006$ ). Thalweg scour and unit scour were both greater at cross sections with greater bed slope, along narrowing valley reaches, where bedrock was exposed on one or both sides of the channel. Shear stress and unit stream power both increase with increased slope. Unit stream power also increases as the valley width decreases for a given discharge. Thus the capacity of the flow to entrain and transport sediment are greater with increasing bed slope and along reaches with narrowing valleys. Basin scale attributes explained a significant portion of the net channel change that was measured and, to a lesser degree, the amount of fill recorded at the cross sections. Unit fill and net fill at cross sections was greater with distance downstream and drainage area above the cross sections. These patterns are largely driven by the tremendous amount of aggradation recorded in the portion of the wash furthest downstream.

In summary, thalweg change and unit scour were best explained at the reach scale and net change and unit fill were best explained at the basin scale. These findings are consistent with the multiple regression analyses above, but indicate that the attributes of the cross section (percent cover of vegetation, number of channels, and valley width) and basin (distance downstream and contributing drainage area) play a less significant role in determining cross section response to flooding than do reach scale attributes such as the valley slope and variations in valley width through the reach.

### *Classification of Cross Sections Based on Physical Attributes*

Cluster analysis resulted in four groups of cross sections (Figure 12). The range in cluster attributes is similar to that described by Ayres Associates (1996), but inclusion of a cross section in a cluster in this analysis was based on multiple characteristics of each cross section: valley slope, valley width, rate of change in valley width, presence or absence of bedrock, and the proportion of the cross section vegetated. This objective clustering resulted in groupings that differed slightly from the Ayres Associates groupings, but the general downstream trends described by Ayres Associates are nonetheless the general trend (Table 7).

The first cluster includes three cross sections: cross sections 18, 21, and 25. This cross section type has narrow valleys (average valley width 163 m) which are confined by bedrock along one or both sides. These cross sections have from three to five split flow paths, average vegetation cover of 30%, and valley slopes of 0.021 m/m. Water surface width during hurricane

related flows averaged 77 m at these cross sections and average width/depth ratio was 202. Average flow depth was 39 cm and maximum flow depth was 92 cm. These cross sections all aggraded during flooding from Hurricane Nora and thalwegs filled by an average of 9 cm.

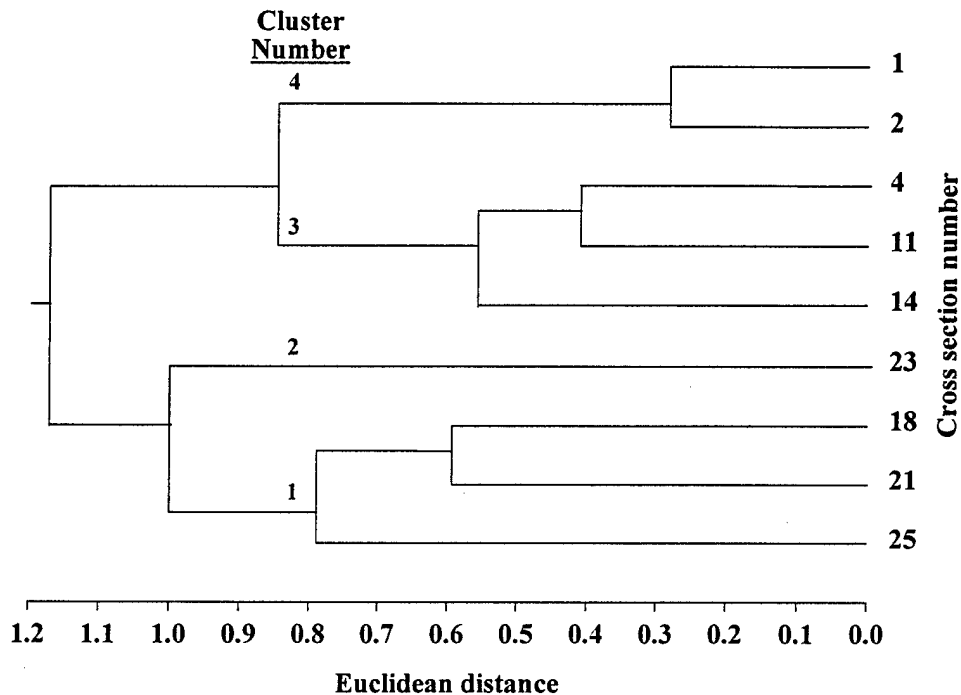


Figure 12. Dendrogram of cluster analysis of cross sections. Agglomerative cluster analysis using average Euclidean distance was used to cluster cross sections based on similarities in several physical attributes: valley slope, valley width, rate of change in valley width, presence or absence of bedrock, and the proportion of the cross section vegetated. This figure may be interpreted as follows. Cross section 1 and 25 are the least similar of all cross sections based on their physical attributes. Cross sections 18 and 21 are more similar to one another than either are to cross section 25, but the three of them are more similar to one another than to any other cross section.

The second cluster contains only one cross section, cross section 23. Slope and valley width of this cross section are similar to the previous cluster, 0.023 m/m and 159 m, respectively, but vegetation cover was more than twice that of the last group of cross sections (67% cover). Width/depth ratio of cross section 23 was 368. This cross section degraded and the thalweg scoured during Hurricane Nora.



Table 7. Comparison of cross section classification by Ayres Associates in which cross sections were subjectively grouped according to reach type, and an objective classification using agglomerative clustering based upon physical attributes of each cross section: valley slope, valley width, rate of change in valley width, presence or absence of bedrock, and the proportion of the cross section vegetated. Asterisk superscript in channel change column indicates that the cross section was correctly classified as aggraded or degraded by a discriminant function using the hydraulic variable maximum depth of flow during the Hurricane Nora flood.

|            | Cross<br>Section | Ayres Associates<br>Reach Type | Cluster | Channel<br>Change |
|------------|------------------|--------------------------------|---------|-------------------|
| upstream   | 25               | 1                              | 1       | aggraded          |
|            | 23               | 1                              | 2       | degraded*         |
|            | 21               | 1                              | 1       | aggraded*         |
|            | 18               | 2                              | 1       | aggraded*         |
|            | 14               | 2                              | 3       | degraded*         |
|            | 11               | 3                              | 3       | degraded*         |
|            | 4                | 3                              | 3       | aggraded*         |
|            | 2                | 4                              | 4       | aggraded*         |
| downstream | 1                | 4                              | 4       | aggraded*         |

The third cluster of cross sections includes three cross sections, cross sections 4, 11, and 14. These cross sections are located in valleys of intermediate width (average 211 m), with little bedrock confinement, and 4 to 7 split flow paths. These cross sections have lower valley slopes than any other cluster, averaging 0.019. Average vegetation cover at these cross sections is 24% and valley walls widen along these reaches. Water surface width during the peak flow of Hurricane Nora averaged 138 m at these cross sections, average width/depth ratio was 315, and average and maximum depth of flow were 43 cm and 97 cm, respectively. Two of the cross sections in this cluster aggraded, whereas the third and furthest downstream cross section (cross section 4) aggraded significantly.

The fourth cluster in this analysis includes cross sections 1 and 2, the furthest downstream of all cross sections, and nearest the confluence of the wash and the Colorado River. Valley widths average 426 m in this cluster. Width/depth ratio is higher than any other cluster, averaging 681. Valley slope averages 0.020 for this cluster and both valleys widen downstream through the reach. Vegetation cover averages 26% in cross sections in this cluster. Both cross sections in this cluster aggraded (average 12 m<sup>2</sup>) and one thalweg scoured 30 cm, whereas the other experienced no change in depth.

## Conclusions

Flows associated with Hurricane Nora ranged from  $16 \text{ m}^3/\text{s}$  to  $237 \text{ m}^3/\text{s}$ , increasing rapidly with distance downstream in the wash. Hurricane-related flooding caused extensive flooding along re-surveyed cross sections, particularly in the lower reaches of Yuma Wash, where discharge was nearly 15 times that estimated for cross sections in the upper reaches of the wash. The frequency of storms of the magnitude of Hurricane Nora is approximately once every 3 years. Flows in Yuma Wash may have been of greater magnitude during Hurricane Nora than flows during the average three year rainfall due to higher antecedent moisture from successive rainstorms prior to September 25, 1998. Discharge associated with a less frequent, higher magnitude historic flood was estimated to be on the order of five times larger than flows associated with Hurricane Nora, and is suspected to have been associated with rain storms recorded in 1972. The magnitude of the 1972 storm (76 mm in a single day) is the largest on record. The recurrence interval of such an event, which generated an estimated flow of greater than  $1280 \text{ m}^3/\text{s}$ , is approximately 40 years. This flow is a reasonable estimate of the probable maximum flood in Yuma Wash.

The flooding associated with Hurricane Nora resulted in extensive channel change at some re-surveyed cross sections throughout the 19.2 km length of Yuma Wash surveyed. Channel change ranged from a maximum of  $-10 \text{ m}^2$  of degradation to  $33 \text{ m}^2$  of channel aggradation. The average degradation of cross sections that experienced net scour was  $-6 \text{ m}^2$ , whereas cross sections that aggraded during Hurricane Nora filled by an average of  $12 \text{ m}^2$ . There were alternating reaches of degradation and aggradation throughout the wash, suggesting the propagation of a sediment wave, which may be moving downstream over the course of several floods. Continued re-surveys following subsequent floods are necessary to confirm this hypothesis. Alternative explanations for this wave-like pattern include differential upland sources of sediment corresponding to different reaches of the wash and/or spatial variability of precipitation and flood wave propagation within sub-basins of the wash.

Physical characteristics of the wash that best explain aggradation and degradation at re-surveyed cross sections include the number of split flow paths or individual channels at a cross section and the width of the valley. Given these two variables, discriminant functions accurately classified 67% of the cross sections as aggraded or degraded. Hydraulic variables estimated from high water marks deposited by the flood were the best predictors of whether a cross section aggraded or degraded, as well as the degree of scour or fill at a particular cross section. Discriminant functions and regression equations using one hydraulic variable, maximum depth of flow during Hurricane Nora, resulted in 89% correctly classified cross sections (aggraded or degraded) and explained 79% of the amount of scour and fill measured at the re-surveyed cross sections, respectively. Unit fill (fill/width of cross section) was best explained by the average flow depth at the cross sections ( $r^2 = 0.63$ ).

Channel change during Hurricane Nora was best explained at the reach scale. Reach scale attributes included valley slope and rate of change in valley width. Steeper valleys with

narrowing valley walls tended to respond to the discharge generated by Hurricane Nora by degrading, and less steep valleys with parallel or widening valley walls tended to aggrade. Thalweg scour was higher along cross sections with higher vegetation cover and lower average depth during flooding. This suggests that if flow depth is insufficient to flood vegetated bars, flow may be confined to active channels which scour during floods. At higher flows, when bars are flooded, the hydraulic roughness associated with the vegetation results in net aggradation of cross sections through vertical accretion of vegetated bars. These results suggest that valley segments respond in predictably different ways to similar patterns of flooding. This also implies that some valley segments may be more or less sensitive to human activities than others. During exceptionally large flow events, or events such as Hurricane Nora in which flow increases exponentially downstream, vegetation stabilizes ridges between split-flow channels and facilitates the retention and storage of sediment in the system. During frequent floods of low magnitude, vegetated bars confine flow to a portion of the channel, resulting in scouring and channel degradation. Further investigation is necessary to verify these hypotheses.

#### *Implications for Land Management at Yuma Proving Ground*

Other channel features which may play an important role in sediment mechanics of Yuma Wash but were not measured as a part of this research include: fine root layers, cryptogamic crusts, armoring layers of coarse bed material or desert pavements, and subsurface crust layers comprised of carbonates or sulphates. Each of these features were observed in Yuma Wash, but measurement of the distribution, extent, and importance of these features was beyond the scope of this study. Other studies have demonstrated that each of these features contribute to stabilization and permeability of soils in arid regions. Fine roots were shown to increase soil structure and to increase water permeability of semi-arid sodic soils in India (Singh 1998). Cryptogamic soils, which inhibit rainsplash and wind erosion and resist sediment removal by overland flow, were shown to be extremely important in stabilizing desert soils in experimental plots by Williams et al. (1995). Schick et al. (1987) discusses the importance of armoring of bed material in the mechanics of bedload transport in ephemeral streams in Israel. Subsurface carbonate layers, which require on the order of  $10^4$  years to form duricrusts, may be highly resistant to scouring during floods (Cooke et al. 1993). All of these features, while resistant to flood related disturbance, may be substantially altered by human activities such as vehicle use. The modifications of these stabilizing features or the vegetated ridges that were described above, could cause much more significant channel responses to flooding than were documented in this study. Although it is difficult to predict the effect of damage to these features on long-term channel changes in Yuma Wash, it is likely that widespread impacts to these features within Yuma Wash would have a significant influence on channel response to change. It has been hypothesized that the destruction of soil stabilizing features and the removal of vegetation may be related to cycles of gully formation and arroyo cutting in ephemeral streams (Cooke and Reeves 1976). Although remedial measures are available to rehabilitate vegetation and fine root layers (Singh 1998) and cryptogamic soil crusts (Buttars et al. 1998), bed armoring, pavements, and carbonate crusts require much longer timescales over which to

form ( $10^2$  -  $10^4$  years). Avoiding significant disturbance to these features is advisable.

Since the late 1800's, the causes of cycles of erosion and aggradation in ephemeral stream systems have remained unresolved. The issue is however of great scientific interest and of certain ecological and economic importance. The incision of channels and the subsequent formation of gullies and arroyos causes the lowering of local and regional groundwater levels, modifications in the cover and composition of groundwater dependent vegetation, and the production and delivery of a tremendous amount of sediment to areas downstream of degrading reaches. The causes of the initiation of erosional and depositional cycles in ephemeral stream systems may be associated with poor land-use (overgrazing, vehicle use, and intentional removal of vegetation), changes in climate, or random variations in the fluvial system (Cooke and Reeves 1976). It is extremely difficult to isolate specific causes of arroyo formation in a system that has already become incised. In contrast, examination of systems that are in apparent equilibrium with current climatic and land-use conditions may facilitate an understanding of the fluvial processes in non-degrading systems and aid in developing land-use practices that prevent the initiation of a cycle of incision leading to gully and arroyo formation.

Although a significant redistribution in sediment resulted in some net channel change in Yuma Wash during the hurricane flooding, such change is likely the normal response of an ephemeral system to a relatively frequent, low magnitude flood. The sediment mechanics within such systems are influenced by the depth of flow and the presence of vegetation and possibly organic and mineral crusts and armoring layers. This study documented a few of these influences over the course of a single flood, and isolated several of the controls on the distributions of sediment within Yuma Wash.

## Literature Cited

- Arcement, G.J. and V.R. Schneider. 1987. Roughness coefficients for densely vegetated flood plains. U. S. Geological Survey Water-Resources Investigations report number WRI 83-4247, Reston, VA. 62 p.
- Ayres Associates. 1996. Geomorphic, hydrologic, and vegetation base-line conditions of Yuma Wash, Yuma Proving Grounds, Arizona. Unpublished report prepared for Waterways Experiment Station, U.S. Army Corps of Engineers, Vicksburg, Mississippi and Conservation Program, U.S. Army, Yuma Proving Ground, Yuma, Arizona.
- Begin, Z.B. and M. Inbar. 1984. Relationship between flows and sediment size in some gravel streams of the arid Nagev, Israel in E.H. Koster and R.J. Steel eds. *Sedimentology of Gravels and Conglomerates*. Canadian Society of Petroleum Geologists, Memoir 10:69-75.
- Buttars, S.M., J.R. Johansen, J.C. Sray, M.C. Payne, B.L. Webb, R.E. Terry, B.K. Pendleton, and S.D. Warren. 1998. Pelletized cyanobacterial soil amendments: laboratory testing for survival, escapability, and nitrogen fixation. *Arid Soil Research and Rehabilitation* 12:165-178.
- Clapp, E.M. and P.B. Bierman. 1998. Estimating long-term erosion rates in a hyper-arid region using in situ produced cosmogenic <sup>10</sup>BE and <sup>26</sup>AL in sediment and Bedrock. Paper presented at The Geological Society of America 1998 Annual Meeting, Toronto, Canada, October 1998. Abstracts with Programs 30:A361.
- Cooke, R.U. and R.W. Reeves. 1976. *Arroyos and environmental change in the American Southwest*. Oxford University Press, Oxford, England, 213 p.
- Cooke, R., A. Warren, and A. Goudie. 1993. *Desert Geomorphology*. University College London Press, London, England, 526 p.
- Cowan, W.L. 1956. Estimating hydraulic roughness coefficients. *Agricultural Engineering* 37:473-475.
- Graf, W.L. 1987. Late Holocene sediment storage in Canyons of the Colorado Plateau. *Geological Society of America Bulletin* 99:261-271.
- Graf, W.L. 1988. *Fluvial Processes in Dryland Rivers*. Springer-Verlag, Germany.
- HEC 1996. HEC-RAS River Analysis System version 1.1 software, developed by U.S. Army Corps of Engineers, Hydrologic Engineering Center, Davis, CA.
- Hermann Zillgens Associates. 1992. Environmental Assessment Report, Target Recognition Range, Yuma Proving Ground, Arizona. Unpublished report prepared for Sacramento District U.S. Army Corps of Engineers, 39 p.
- House, P.K. 1997. An unconventional, multidisciplinary approach to evaluating the magnitude and frequency of flash floods in small desert watersheds. Arizona Geological Survey Open File Report 97-9, Reno, NV, 46 p.
- Inbar, M. and A.P. Schick. 1979. Bedload transport associated with high stream power, Jordan River, Israel. *Proceeding of the National Academy of Sciences* 76:2515-2517.
- Knighton, D. 1984. *Fluvial Forms and Processes*. Edward Arnold, London, 218 p.

- Kochel, R.C. 1988. Geomorphic impact of large floods: review and new perspectives on magnitude and frequency *in* Flood Geomorphology, V.R. Baker, R.C. Kochel, P.C. Patton eds. John Wiley and Sons, Inc., New York.
- Leopold, L.B. and T. Maddock. 1953. The hydraulic geometry of stream channels and some physiographic considerations. U.S. Geological Survey Professional Paper 252, Washington, D.C., 57 p.
- Leopold, L.B. and J.P. Miller. 1956. Ephemeral Streams-Hydraulic Factors and their Relation to the Drainage Net: Physiographic and Hydraulic Studies of Rivers. U.S. Geological Survey Professional Paper 282-A, Washington, D.C., 34 p.
- Madej, M.A. and Ozaki, V. 1996. Channel response to sediment wave propagation and movement, Redwood Creek, California, USA. *Earth Surface Processes and Landforms* 21:911-927.
- NOAA 1998. National Oceanic and Atmospheric Administration NCDC Summary of the Day Weather Data, published by EarthInfo, Inc., Boulder, CO.
- Phillips, J.V. and T.L. Ingersoll. 1998. Verification of roughness coefficients for selected natural and constructed stream channels in Arizona. U.S. Geological Survey Professional Paper 1584, Washington, D.C., 77 p.
- Phillips, J.V. D. McDoniel, J.P. Capesius, and W. Asquith. 1998. Method to estimate effects of flow-induced vegetation changes on channel conveyances of streams in central Arizona. U.S. Geological Survey Water Resource Investigations Report 98-4040, Washington, D.C., 43 p.
- Rappaport, E.N. 1997. Hurricane Nora 16-26 September 1997. National Hurricane Center unpublished report, National Oceanic and Atmospheric Administration.
- Schick, A.P. 1970. Desert floods—interim results of observations in the Nahal Yael Research Watershed, Southern Israel, 1965-1970. IAHS-Unesco Symposium on the Results of Research on Representative and Experimental Basis, Wellington, NZ.
- Schick, A.P., J. Lekach, and M.A. Hassan. 1987. Bedload transport in desert floods: observations in the Nagev *in* Sediment Transport in Gravel-bed Rivers, C.R. Thorne, J.C. Bathurst, and R.D. Hey eds. John Wiley and Sons Ltd., New York.
- Schick, A.P. 1988. Hydrologic aspects of floods in extreme arid environments *in* Flood Geomorphology, V.R. Baker, R.C. Kochel, P.C. Patton eds. John Wiley and Sons, Inc., New York.
- Schumm, S.A. 1960. The shape of alluvial channels in relation to sediment type. U.S. Geological Survey Professional Paper 352-B, Washington, D.C., 29 p.
- Singh, B. 1998. Contribution of forest fine roots in reclamation of semiarid sodic soils. *Arid Soil Research and Rehabilitation* 12:207-222.
- Strickler, A. 1923. Beitrage zur Frage der Geschwindigkeitsformel und der Rauhigkeitszahlen fur Strome, Kanale und geschlossene Leitungen. Mitt Eidgen Amt Wasserrwirtsch, Bern.
- Trieste, D.J. and R.D. Jarrett. 1987. Roughness coefficients of large floods. Irrigation and Drainage Division Specialty Conference Proceedings, L.G. James and M.J. English eds. American Society of Civil Engineers, New York. p. 32-40.

USDI 1995. Scour and Fill version 7.1 software, U.S. Department of Interior, National Biological Service, Arcata, CA.

Wende, R. and G.C. Nanson. 1998. Anabranching rivers: ridge-form alluvial channels in tropical northern Australia. *Geomorphology* 22:205-224.

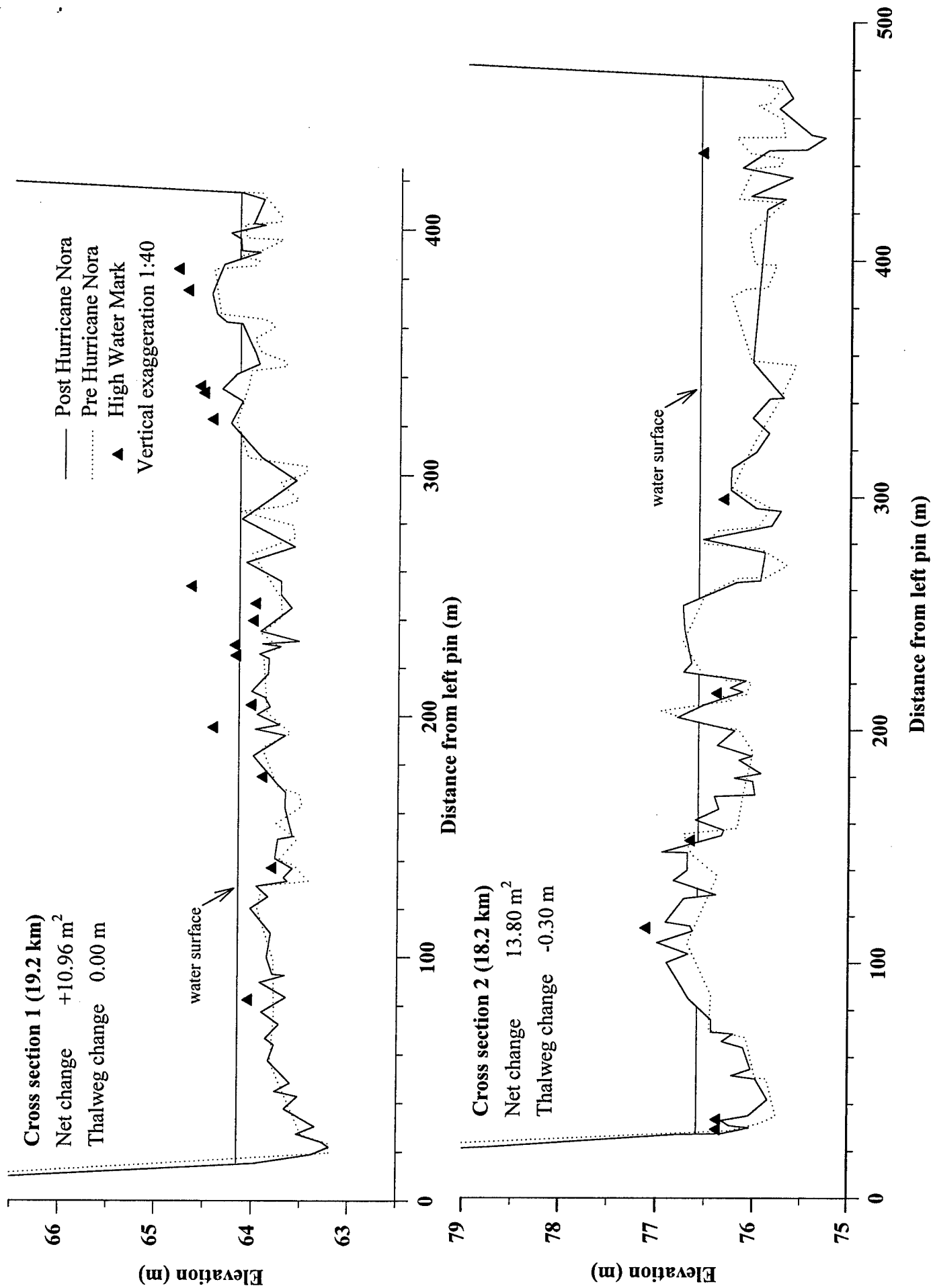
Wilson, E.D. 1960. Geologic map of Yuma County, Arizona. Prepared by the Arizona Bureau of Mines, University of Arizona, Tucson.

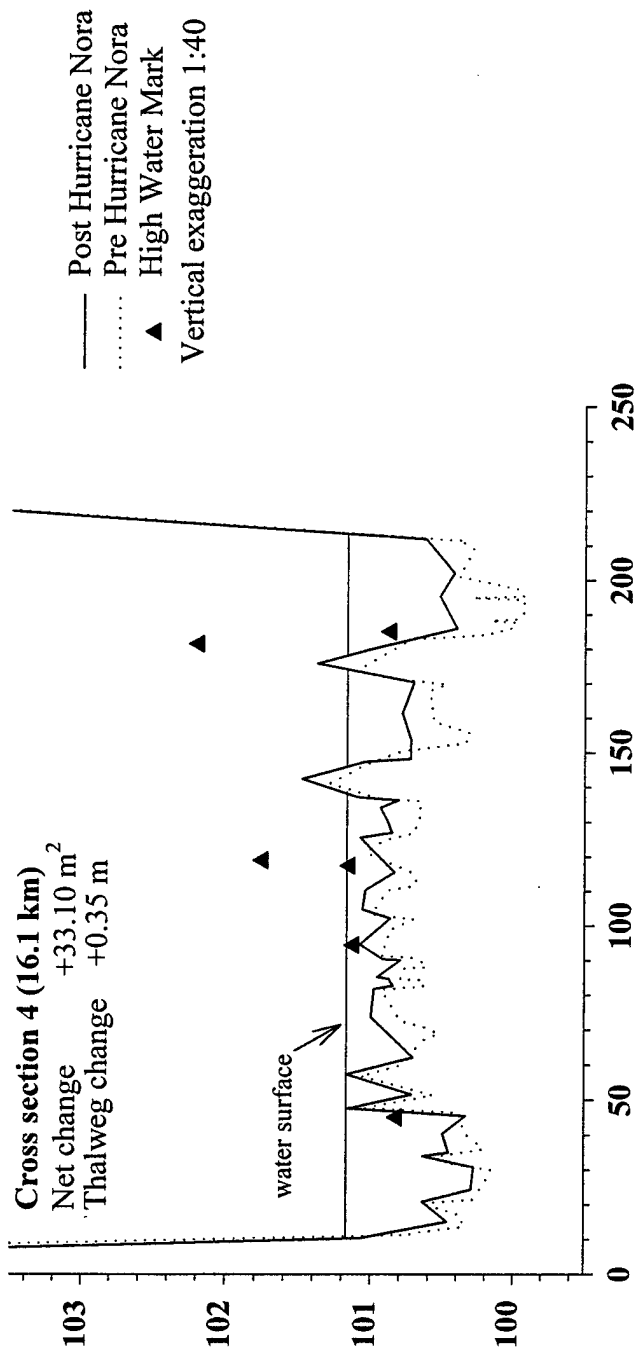
Williams, J.D., J.P. Dobrowolski, and N.E. West. 1995. Microphytic crust influence on interrill erosion and infiltration capacity. *Transactions of the American Society of Agricultural Engineers* 38:139-146.

Young, D.F., B.R. Munson, and T.H. Okiishi. 1997. *A Brief Introduction to Fluid Mechanics*. John Wiley and Sons, Inc., New York.

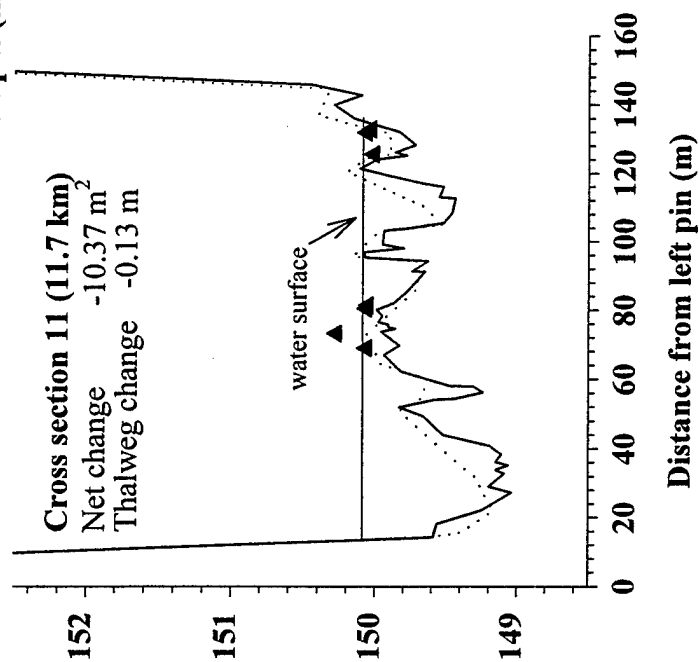
## Appendix I: Re-Surveyed Cross Sections, Yuma Wash

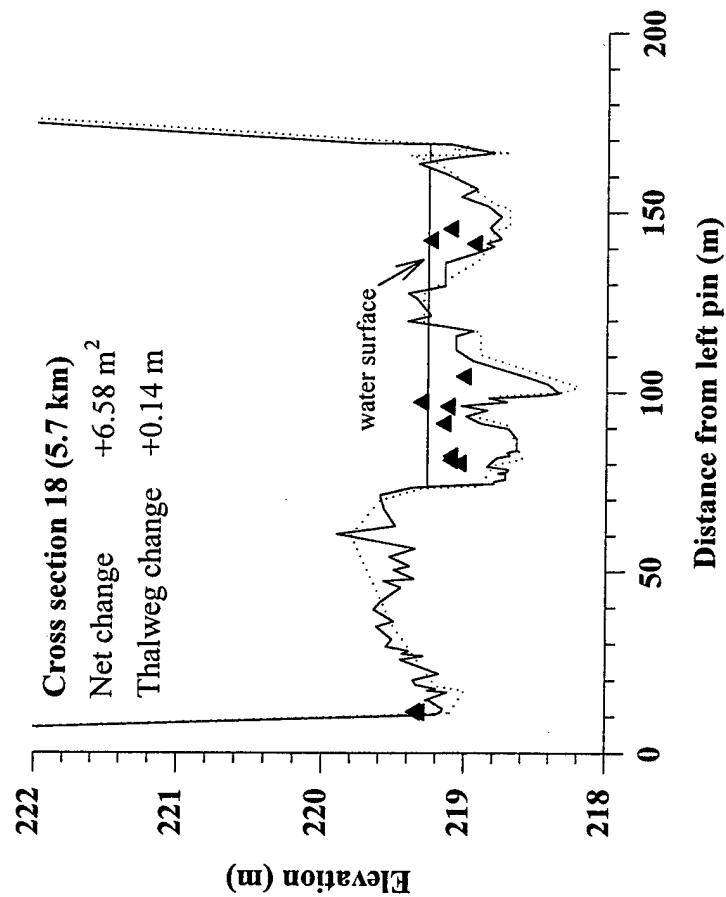
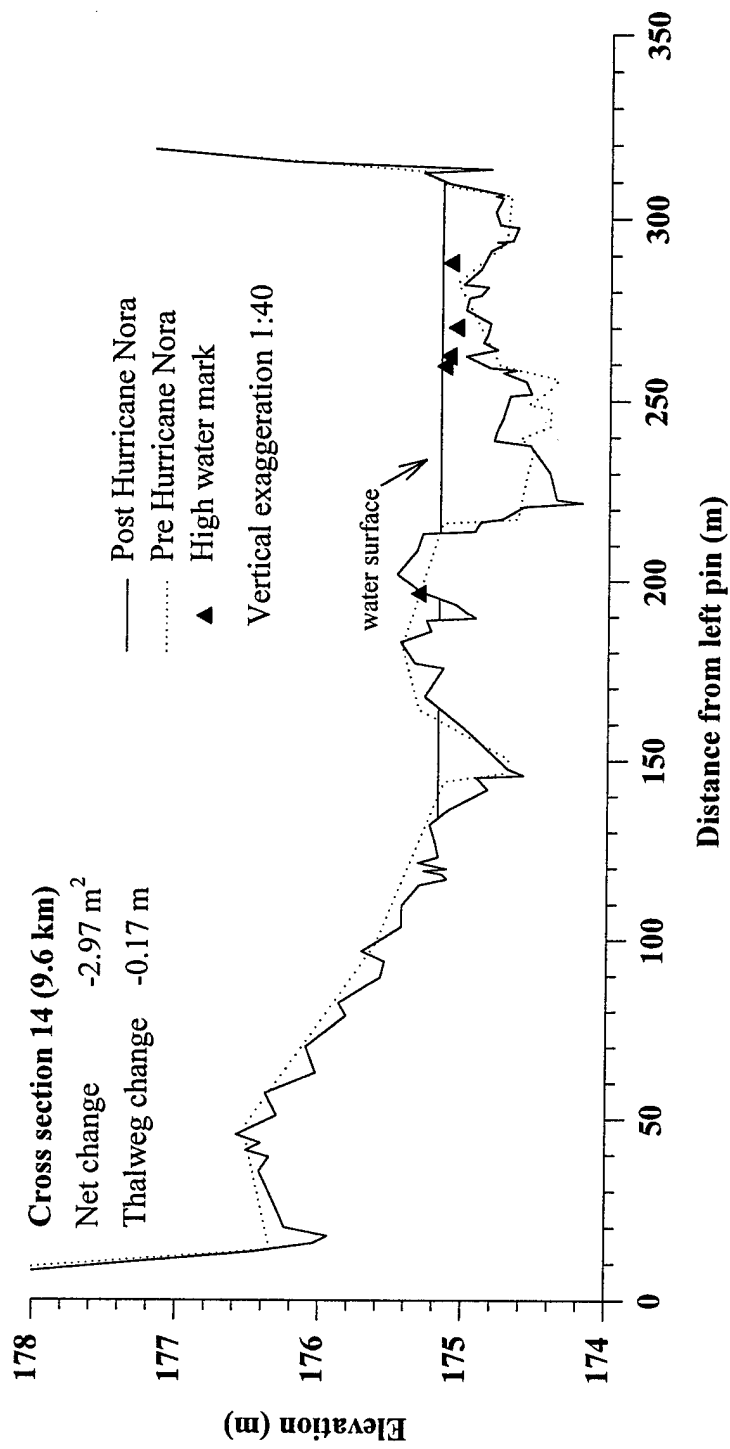


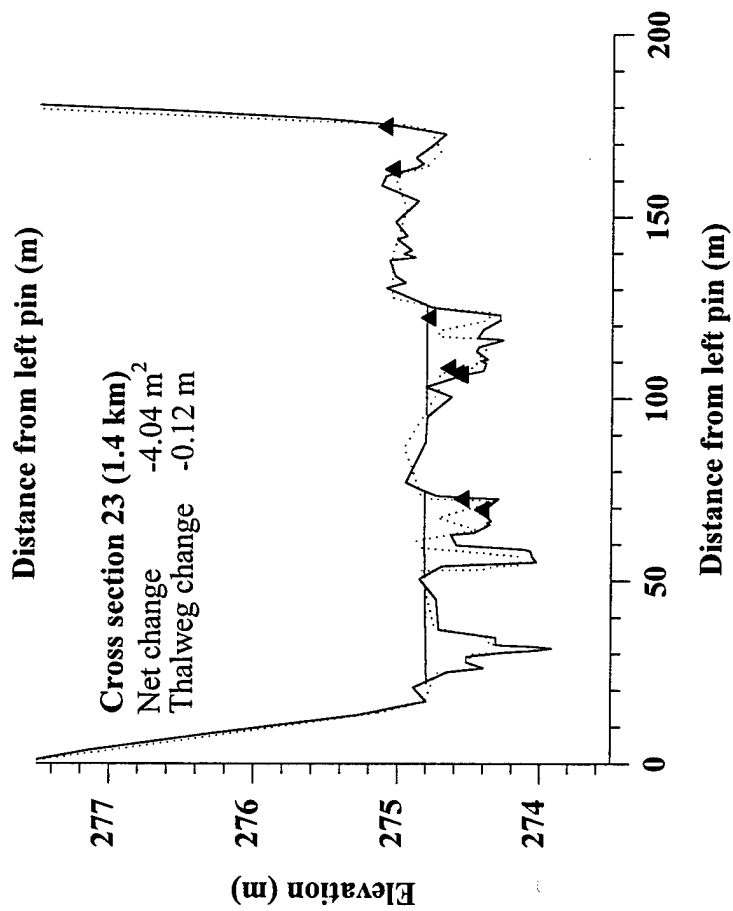
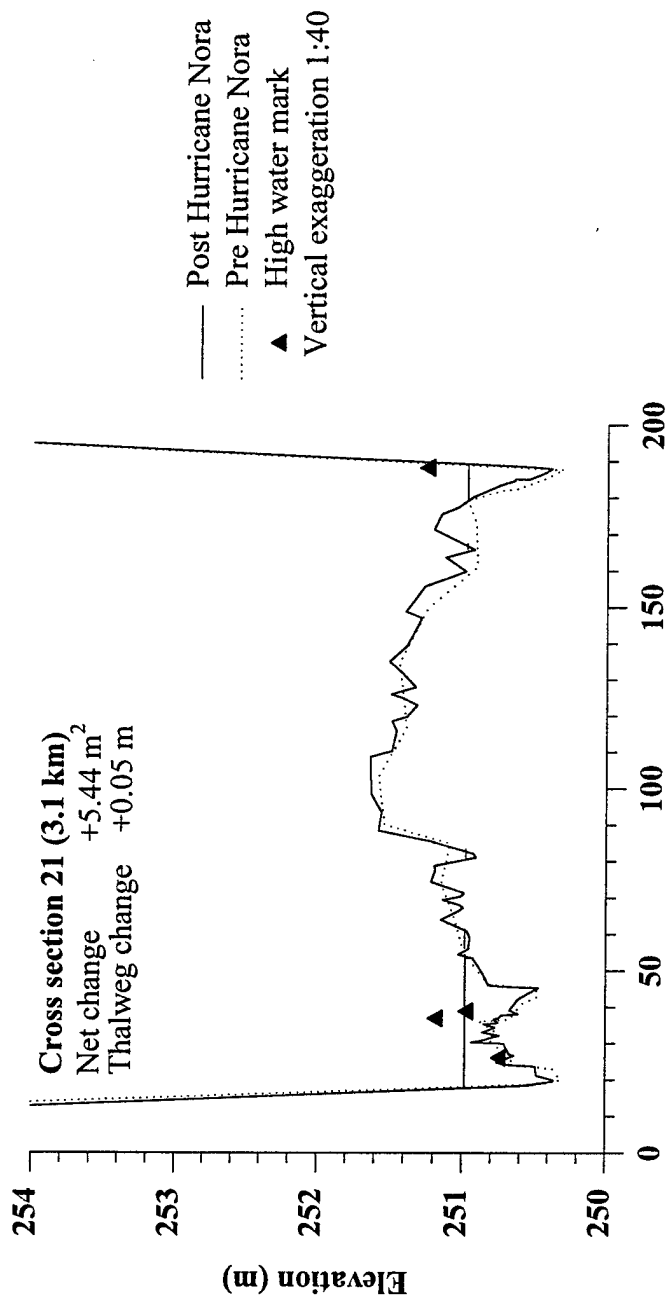


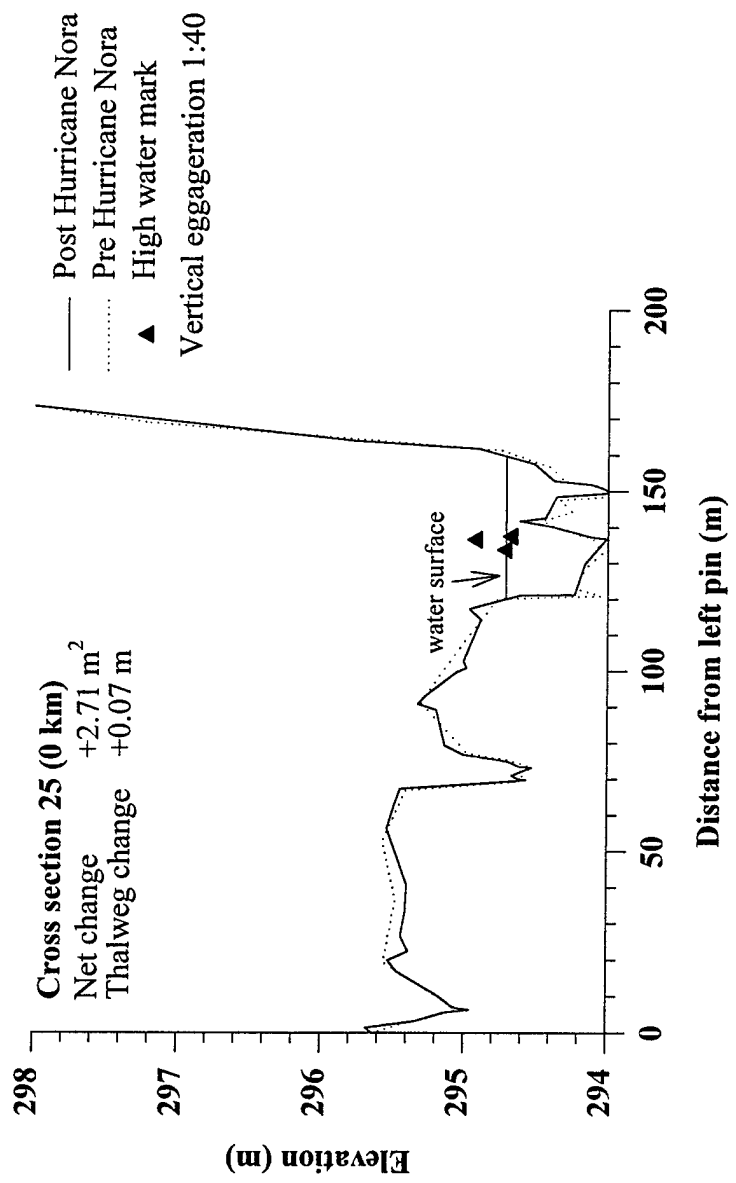


Distance from left pin (m)









## Appendix II: Paired Photographs of Re-surveyed Cross Sections, Yuma Wash

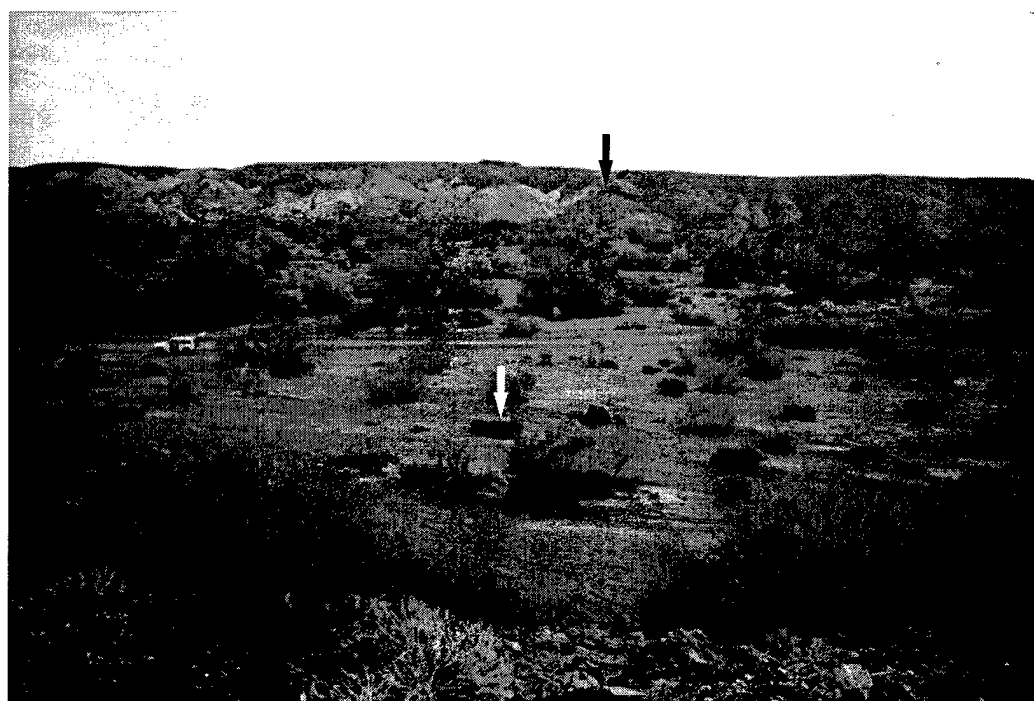
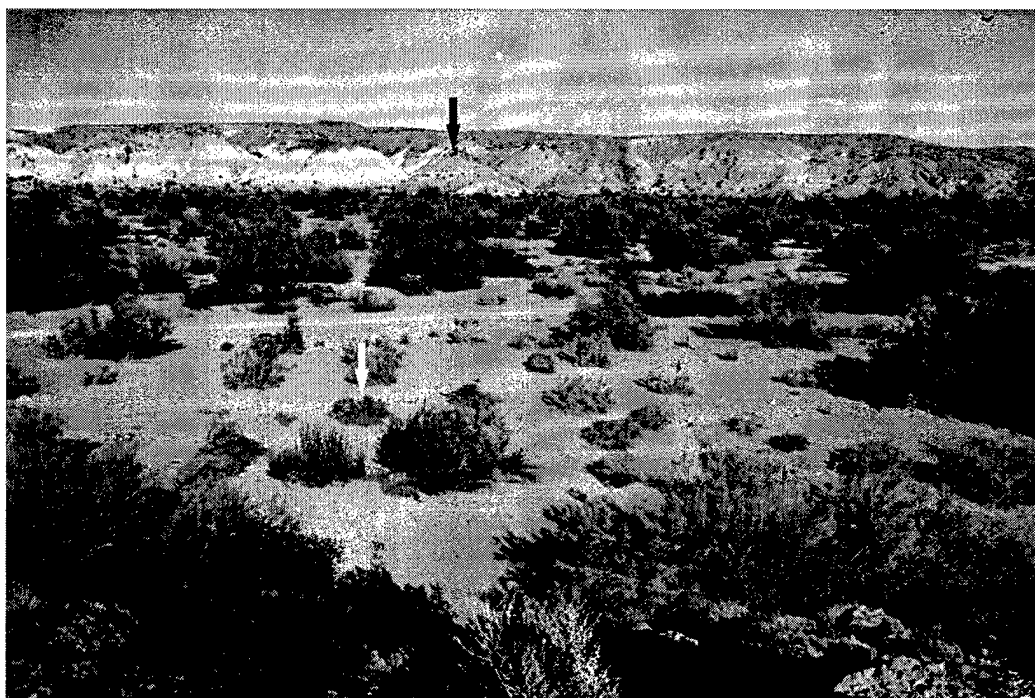


Plate 1. Cross section 1 looking toward river left from river right station. Upper photograph taken by Ayres Associates in 1995, lower photograph taken as a part of this study in 1998. Arrows indicate points of reference.

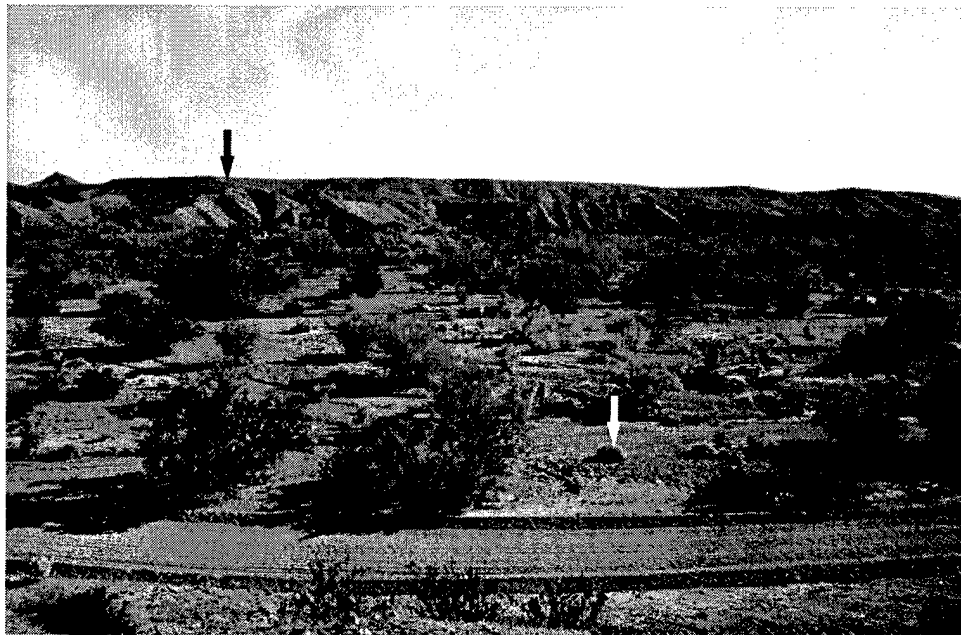
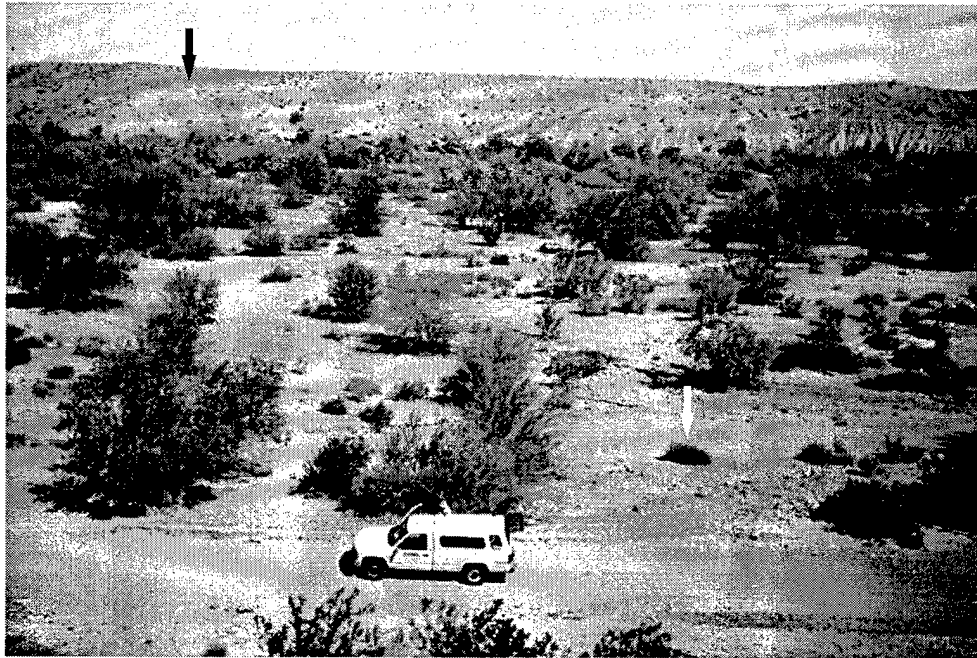


Plate 2. Cross section 2 looking toward river right from river left station. Upper photograph taken by Ayres Associates in 1995, lower photograph taken as a part of this study in 1998. Arrows indicate points of reference.





Plate 3. Cross section 4 looking toward river left from river right station. Upper photograph taken by Ayres Associates in 1995, lower photograph taken as a part of this study in 1998. Arrows indicate points of reference.

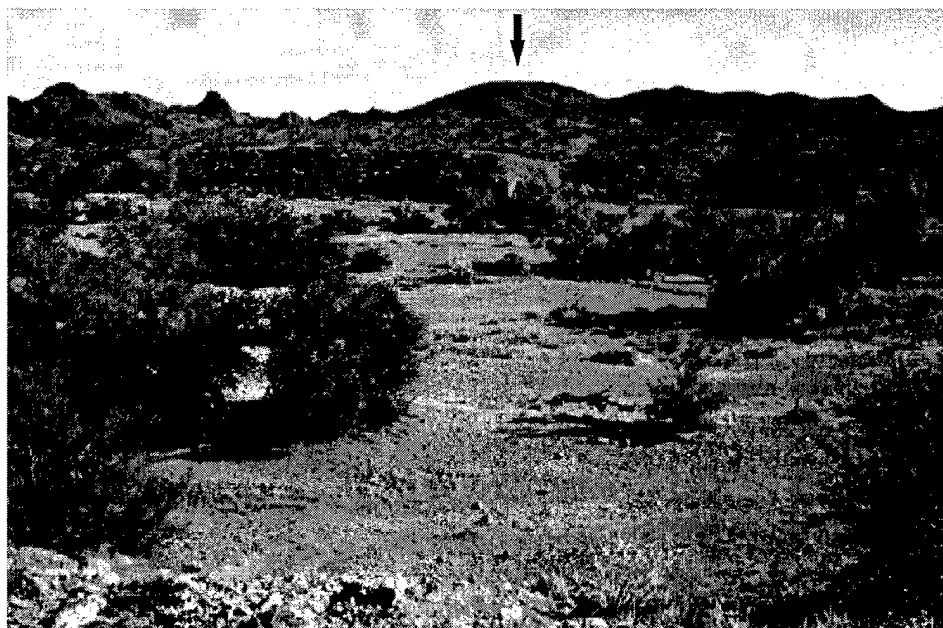


Plate 4. Cross section 11 looking toward river left from river right station. Upper photograph taken by Ayres Associates in 1995, lower photograph taken as a part of this study in 1998. Arrows indicate points of reference.

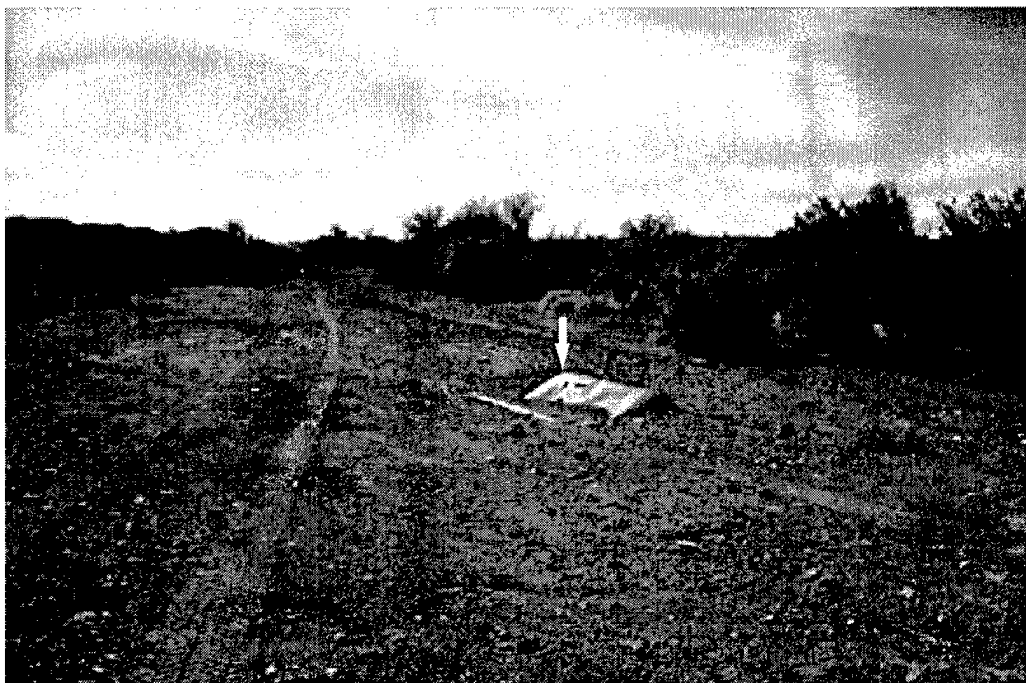
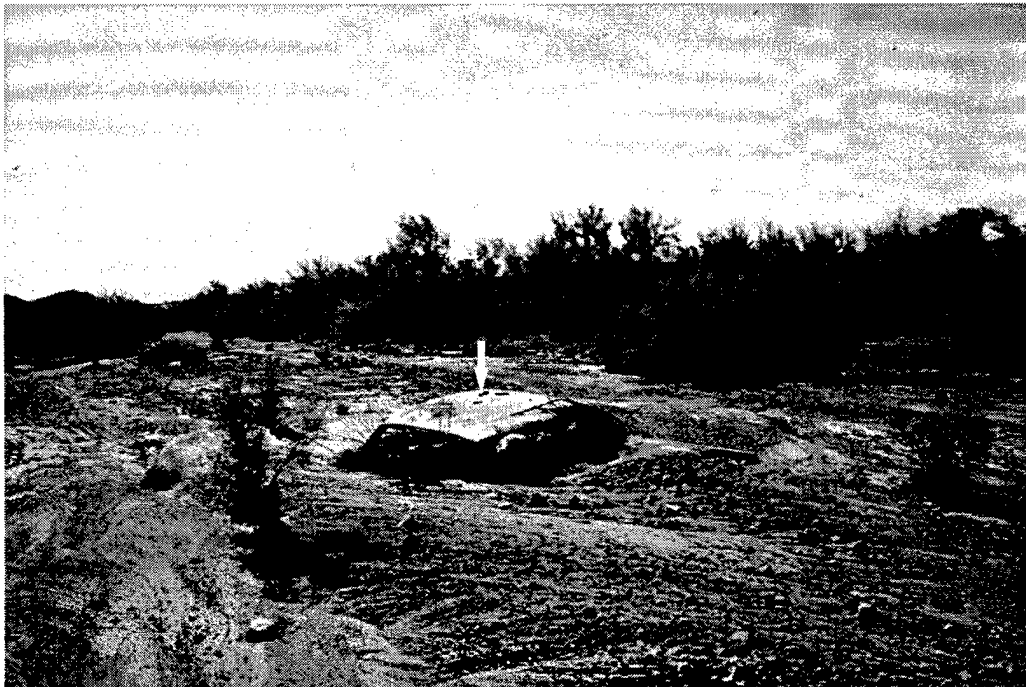


Plate 5. Cross section 14 looking downstream at target car. Upper photograph taken by Ayres Associates in 1995, lower photograph taken as a part of this study in 1998. Arrows indicate points of reference. Note the amount of fill around car.

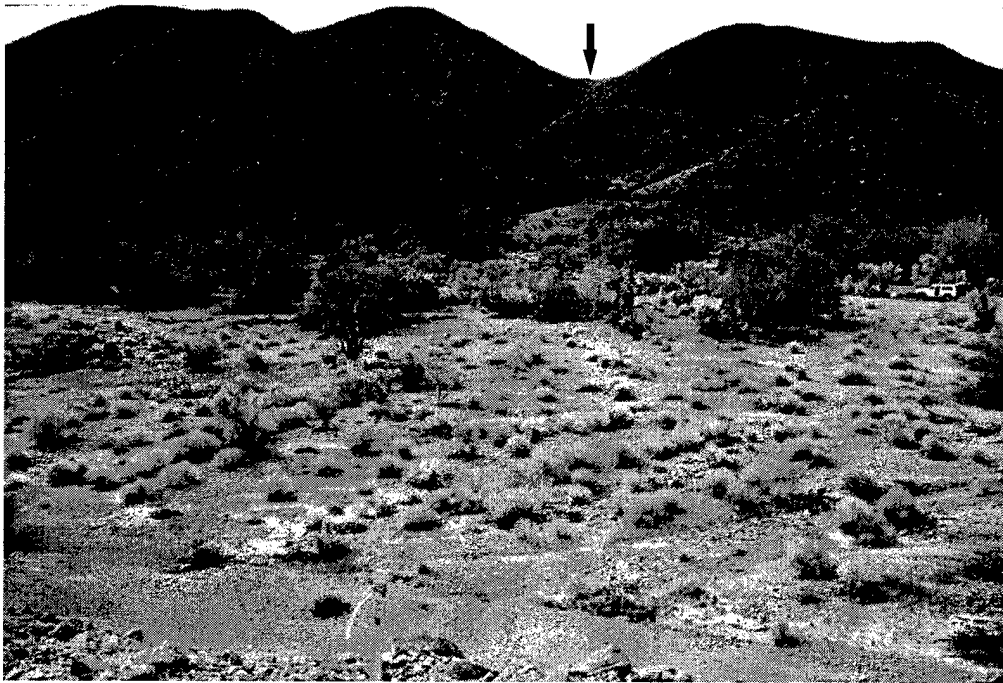


Plate 6. Cross section 18 looking toward river right from river left station. Upper photograph taken by Ayres Associates in 1995, lower photograph taken as a part of this study in 1998. Arrows indicate points of reference.

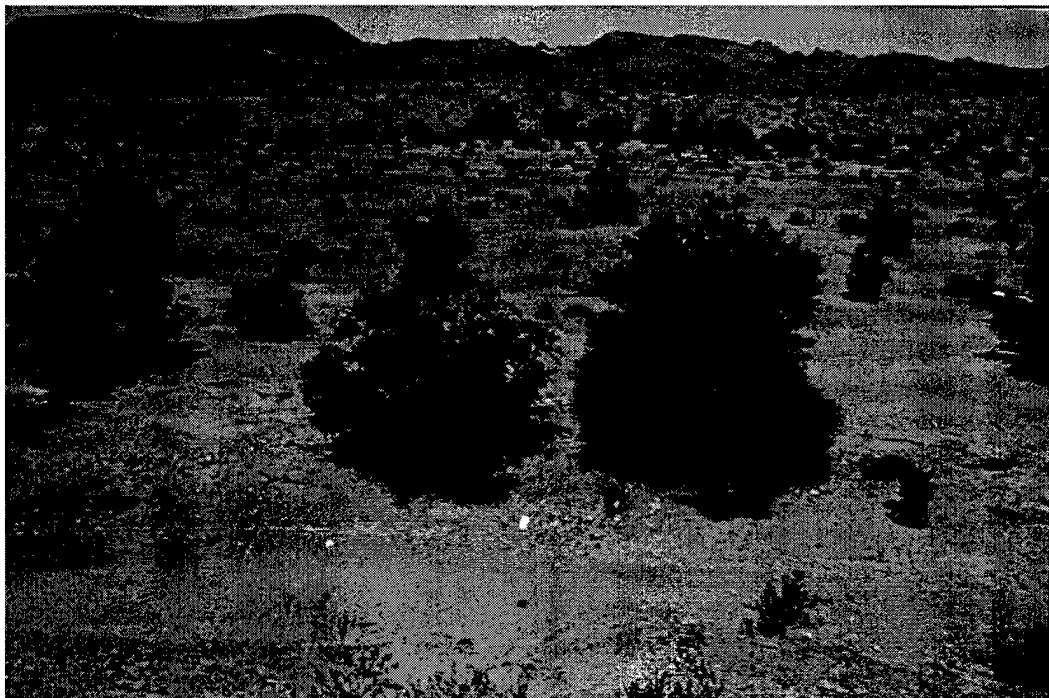


Plate 7. Cross section 21 looking downstream from river right. Upper photograph taken by Ayres Associates in 1995, lower photograph taken as a part of this study in 1998. These photographs are not paired.





Plate 8. Cross section 23 looking upstream from river left. Upper photograph taken by Ayres Associates in 1995, lower photograph taken as a part of this study in 1998. Arrows indicate points of reference.

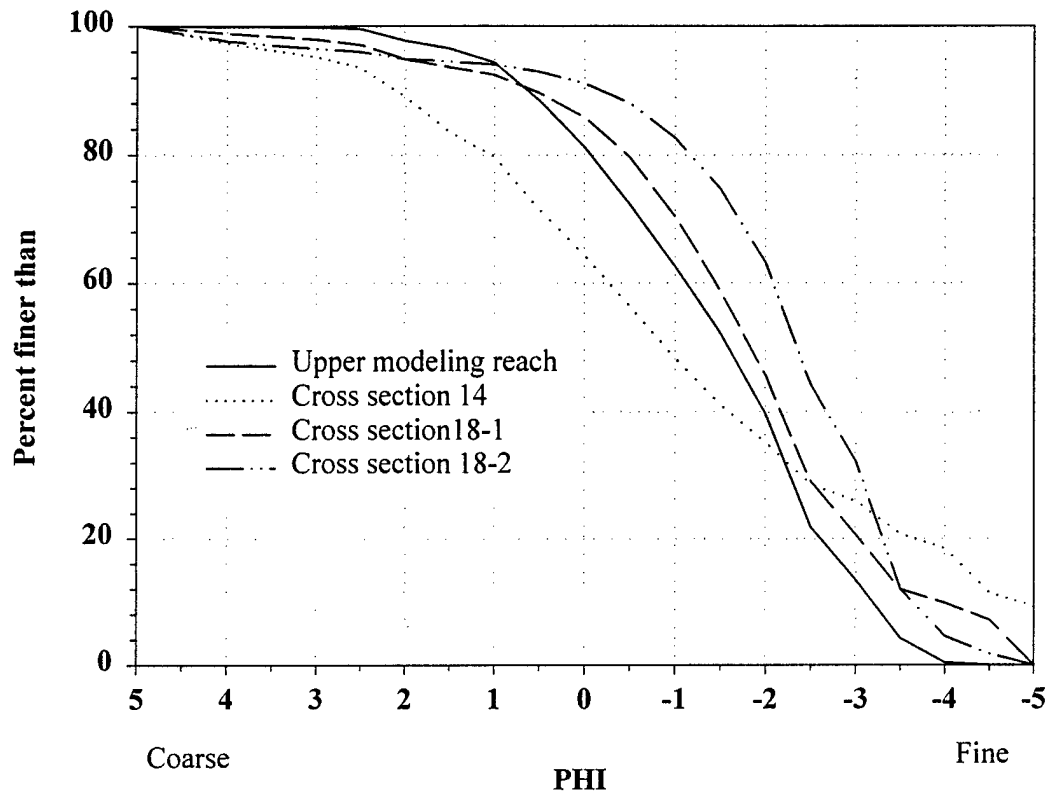


Plate 9. Cross section 25 looking toward river right from to river left station. Upper photograph taken by Ayres Associates in 1995, lower photograph taken as a part of this study in 1998. Arrows indicate points of reference.

### Appendix III: Grain Size Distributions, Yuma Wash



# **Yuma Wash Particle Size Analysis**



Appendix III Figure 1. Particle size distributions for samples from modeled reaches in Yuma Wash.

Appendix III Table 1: Phi values and grain size summary statistics for Yuma Wash.

| Cross section        |     | D <sub>16</sub> | D <sub>25</sub> | D <sub>50</sub> | D <sub>84</sub> |
|----------------------|-----|-----------------|-----------------|-----------------|-----------------|
| Upper modeling reach | PHI | -2.9            | -2.5            | -1.5            | 0.4             |
|                      | mm  | 7.5             | 5.7             | 2.8             | 0.8             |
| Cross section 14     | PHI | -4.2            | -3.0            | -0.9            | 1.5             |
|                      | mm  | 18.4            | 8.0             | 1.9             | 0.35            |
| Cross section 18 #1  | PHI | -3.5            | -2.8            | -1.9            | 0.2             |
|                      | mm  | 11.3            | 7.0             | 3.7             | 0.9             |
| Cross section 18 #2  | PHI | -3.5            | -3.2            | -2.5            | -0.9            |
|                      | mm  | 11.3            | 9.2             | 5.7             | 1.9             |

## Appendix IV: Data

| Hydraulic Data |                         |                      |                               |                     |                   |                  |                |                               |
|----------------|-------------------------|----------------------|-------------------------------|---------------------|-------------------|------------------|----------------|-------------------------------|
| Cross Section  | Water Surface Width (m) | Wetted Perimeter (m) | Wetted Area (m <sup>2</sup> ) | Hydraulic Depth (m) | Maximum Depth (m) | Hydraulic Radius | Velocity (m/s) | Discharge (m <sup>3</sup> /s) |
| XS-25          | 47.1                    | 47.4                 | 19.9                          | 0.42                | 0.79              | 0.42             | 1.88           | 37                            |
| XS-23          | 77.2                    | 76.2                 | 16.0                          | 0.21                | 0.74              | 0.21             | 1.18           | 19                            |
| XS-21          | 90.9                    | 63.6                 | 14.0                          | 0.36                | 0.93              | 0.22             | 1.16           | 16                            |
| XS-18          | 94.2                    | 95.8                 | 36.4                          | 0.39                | 1.04              | 0.38             | 1.60           | 58                            |
| XS-14          | 108.4                   | 107.0                | 42.8                          | 0.39                | 0.78              | 0.40             | 1.65           | 71                            |
| XS-11          | 108.3                   | 110.6                | 39.8                          | 0.37                | 0.89              | 0.36             | 1.54           | 61                            |
| XS-4           | 198.0                   | 199.8                | 105.9                         | 0.53                | 1.23              | 0.53             | 1.98           | 210                           |
| XS-2           | 177.8                   | 181.5                | 85.3                          | 0.48                | 0.97              | 0.47             | 1.88           | 161                           |
| XS-1           | 376.8                   | 376.3                | 143.0                         | 0.38                | 0.99              | 0.38             | 1.66           | 237                           |

| Hydraulic Data (continued) |                                  |                        |   |                  |               |  |
|----------------------------|----------------------------------|------------------------|---|------------------|---------------|--|
| Cross Section              | Shear Stress (N/m <sup>2</sup> ) | Stream Power (watts/m) | Unit Stream Power (watts/m <sup>2</sup> ) | Reynold's Number | Froude Number |  |
| XS-25                      | 93.8                             | 8365                   | 178                                       | 786999           | 0.93          |  |
| XS-23                      | 46.7                             | 4208                   | 55  | 247288           | 0.82          |  |
| XS-21                      | 44.6                             | 3308                   | 36  | 255184           | 0.62          |  |
| XS-18                      | 70                               | 10717                  | 114                                       | 604823           | 0.82          |  |
| XS-14                      | 73.3                             | 12936                  | 119                                       | 657060           | 0.84          |  |
| XS-11                      | 66                               | 11213                  | 104                                       | 551223           | 0.81          |  |
| XS-4                       | 96.6                             | 38306                  | 194                                       | 1047549          | 0.87          |  |
| XS-2                       | 90.7                             | 31042                  | 175                                       | 882410           | 0.87          |  |
| XS-1                       | 75.2                             | 46891                  | 124                                       | 626939           | 0.86          |  |

| Physical Data |                                  |                          |                  |                                |         |             |                    |                             |
|---------------|----------------------------------|--------------------------|------------------|--------------------------------|---------|-------------|--------------------|-----------------------------|
| Cross Section | Drainage Area (km <sup>2</sup> ) | Distance Downstream (km) | Valley Width (m) | Rate of Change in Valley Width | Bedrock | Slope (m/m) | Number of Channels | Percent Cover of Vegetation |
| XS-25         | 8.5                              | 0.0                      | 162              | -0.08                          | 1       | 0.0228      | 3                  | 0.22                        |
| XS-23         | 8.9                              | 1.4                      | 159              | -0.36                          | 0       | 0.0227      | 4                  | 0.67                        |
| XS-21         | 15.8                             | 3.1                      | 170              | -0.11                          | 1       | 0.0207      | 5                  | 0.38                        |
| XS-18         | 62.7                             | 5.7                      | 158              | -0.47                          | 1       | 0.0188      | 4                  | 0.30                        |
| XS-14         | 101.6                            | 9.6                      | 299              | 0.10                           | 0       | 0.0187      | 4                  | 0.26                        |
| XS-11         | 105.6                            | 11.7                     | 130              | 0.29                           | 0       | 0.0187      | 5                  | 0.18                        |
| XS-4          | 174.0                            | 16.1                     | 205              | 0.24                           | 1       | 0.0186      | 7                  | 0.28                        |
| XS-2          | 180.1                            | 18.2                     | 453              | 0.19                           | 0       | 0.0197      | 9                  | 0.24                        |
| XS-1          | 186.2                            | 19.2                     | 399              | 0.12                           | 1       | 0.0202      | 8                  | 0.27                        |

| Channel Change: Scour and Fill Data |                         |                        |                                      |                    |
|-------------------------------------|-------------------------|------------------------|--------------------------------------|--------------------|
| Cross Section                       | Scour (m <sup>2</sup> ) | Fill (m <sup>2</sup> ) | Net Channel Change (m <sup>2</sup> ) | Thalweg Change (m) |
| XS-25                               | -0.22                   | 2.93                   | 2.71                                 | 0.07               |
| XS-23                               | -5.87                   | 1.83                   | -4.04                                | -0.12              |
| XS-21                               | -1.95                   | 7.39                   | 5.44                                 | 0.05               |
| XS-18                               | -1.18                   | 7.76                   | 6.58                                 | 0.14               |
| XS-14                               | -9.71                   | 6.74                   | -2.97                                | -0.17              |
| XS-11                               | -12.62                  | 2.25                   | -10.37                               | -0.13              |
| XS-4                                | -0.92                   | 34.02                  | 33.10                                | 0.35               |
| XS-2                                | -16.96                  | 30.76                  | 13.80                                | -0.30              |
| XS-1                                | -1.13                   | 12.09                  | 10.96                                | 0.00               |

| Discharge Estimates (m <sup>3</sup> /s) |                |                |
|---|----------------|----------------|
| Cross Section                           | Hurricane Nora | Historic Flood |
| XS-25                                   | 37             | 193            |
| XS-23                                   | 19             | 86             |
| XS-21                                   | 16             | 255            |
| XS-18                                   | 44             | 80             |
| XS-14                                   | 72             | 388            |
| XS-11                                   | 61             | 128            |
| XS-4                                    | 210            | 1282           |
| XS-2                                    | 336            | 1226           |
| XS-1                                    | 237            | 1147           |

## Appendix V: SAS Statistics Code

FILENAME yuma.sas: Includes SAS code for Principal Components Analysis and Multiple Regression Analysis.

```
options ps=75 ls=70 ;
data yuma;
infile '~/yuma/yuma.dat';
input Plot $ Dist Drain_A Slope Val_w Rate_vw Bedrock
No_chan Perc_veg Ayr_veg Geom Cluster;
infile '~/yuma/yumhyd.dat';
input Plot $ Wat_wid Wet_A Avg_d Mx_d RScour RFill Net_ch Rh Thal_ch;

if Net_ch>0 then SF='FILL';
if Net_ch<0 then SF='SCOUR';

***NORMALIZE SCOUR AND FILL TO PER UNIT LENGTH***;
Scour=RScour/Wat_wid;
Fill=RFill/Wat_wid;

***Back Calculate Wetted Perimeter***;
Wet_per=Wet_A/Rh;

***CALCULATE VELOCITY, DISCHARGE, SHEAR STRESS AND STREAM POWER***;
V = (Rh**0.667)*(Slope**0.5)/0.045;
Q = V * Wet_A;
Shear=Slope*Rh*9800;
Power=Q*Slope*9800;
UPower=Power/Wat_wid;

***CALCULATE W/D, REYNOLDS AND FROUDE NUMBERS***;
WD=Wat_wid/Avg_d;
Re=(V*Rh*998)/0.001002;
Fr=V/sqrt(Avg_d*9.807);

*****PRINT VARIABLES AND CORRELATION ANALYSIS*****;
Proc print;
var Drain_A Dist Val_w Rate_vw Bedrock Slope No_chan Perc_veg;
id Plot;
title 'Physical Variables';
Proc print;
var Wat_wid Wet_per Wet_A Avg_d Mx_d Rh V Q Shear Power UPower Re Fr;
ID Plot;
title 'Hydraulic Variables';
run;
Proc print;
var RScour RFill Net_ch Thal_ch;
title 'Channel Change';
id Plot;
run;
*Proc corr;
*var Dist Drain_A Slope Val_w Rate_vw Avg_d Mx_d Shear
*Wat_wid Wet_per Perc_veg Net_ch Scour Fill;
run;
```

\*\*\*\*\*PRINCIPAL COMPONENTS ANALYSIS\*\*\*\*\*;

Proc PRINCOMP n=4 out=basin1 noprint;

var Dist Drain\_A ;

title 'PCA: Basin Attributes';

\*Proc PLOT data=basin;

\*plot prin1\*prin2;

run;

data basin;

set basin1;

bPCA1=prin1;

bPCA2=prin2;

run;

Proc PRINCOMP n=4 data=yuma out=reach1 noprint;

var Rate\_vw Slope Bedrock;

title 'PCA: Reach Attributes';

\*Proc PLOT data=reach;

\*plot prin1\*prin2;

run;

data reach;

set reach1;

rPCA1=prin1;

rPCA2=prin2;

run;

Proc PRINCOMP n=4 data=yuma out=xs1 noprint;

var Val\_w Perc\_veg No\_chan ;

title 'PCA: Cross-section Attributes';

\*Proc PLOT data=xs;

\*plot prin1\*prin2;

run;

data xs;

set xs1;

xsPCA1=prin1;

xsPCA2=prin2;

run;

Proc PRINCOMP n=4 data=yuma out=hyd1 noprint;

var Avg\_d Mx\_d V Q Wet\_per Shear Power UPower;

title 'PCA: Hydraulic Attributes';

\*Proc PLOT data=hydra;

\*plot prin1\*prin2;

run;

data hyd;

set hyd1;

hPCA1=prin1;

hPCA2=prin2;

run;

data master;

set yuma;

set basin;

set xs;

set reach;



\*\*\*\*\*REGRESSIONAL ANALYSIS ON VARIABLES\*\*\*\*\*;

```
Proc reg data=yuma;
model Thal_ch Net_ch Scour Fill=Drain_A Dist Slope Val_w Rate_vw
No_chan Perc_veg /selection=stepwise;
title 'Multiple Regression Physical Variables';
run;
```

```
Proc reg data=yuma;
model Thal_ch Net_ch Scour Fill=Avg_d Mx_d V Q Wet_per Shear Power
UPower
WD Fr Re /selection=stepwise;
title 'Multiple Regression Hydraulic Variables';
run;
```

\*BEST REGRESSION MODELS: STEPWISE SELECTION;

```
Proc REG data=yuma;
title 'Critical';
model Thal_ch=Mx_d ;
run;
```

```
Proc REG data=yuma;
model Net_ch=Mx_d ;
run;
```

FILENAME yumclus.sas: Includes SAS code for Cluster Analysis and Discriminant Function Analysis.

```
options ps = 80 ls = 70 nodate;
data yuma;
infile '~/yuma/yuma.dat';
input Plot $ Dist Drain_A Slope Val_w Rate_vw Bedrock
No_chan Perc_veg Ayr_veg Geom Cluster;
infile '~/yuma/yumhyd.dat';
input Plot $ Wat_wid Wet_A Avg_d Mx_d RScour RFill Net_ch Rh
Thal_ch;

Scour=RScour/Wat_wid;
Fill=RFill/Wat_wid;
if Thal_ch>0 then TH='AGG';
if Thal_ch<0 then TH='DEG';
if Thal_ch=0 then TH='NOCH';

if Net_ch>0 then SF='FILL';
if Net_ch<0 then SF='SCOUR';
Proc sort;
by TH;
Proc means;
var Slope Rate_vw Val_w Perc_veg Mx_d Avg_d;
by TH;
run;

***VELOCITY, DISCHARGE, SHEAR STRESS, and STREAM POWER***;
V=((Rh**0.667)*(Slope**0.5))/0.045;
Q=V*Wet_A;
Shear = 9800*Slope*Rh;
Power = 9800*Slope*Q;
WD=Wat_wid/Avg_d;
UPower=Power/Wat_wid;

Proc print;
*Proc corr;
var Slope Val_w Perc_veg TH;
*var Plot Dist Drain_A Slope Val_w Rate_vw Bedrock Avg_d Mx_d No_chan
Wat_wid Wet_per Perc_veg Net_ch Scour Fill;
id Plot;
run;

****CLUSTER ANALYSIS****;

*Proc FREQ;
*tables cluster*SF;
*run;

*Proc CANDISC data=yumaclus out=can;
*class cluster;
*var Dist Drain_A Slope Val_w Rate_vw Bedrock Avg_d Mx_d No_chan
*Wat_wid Wet_per Perc_veg ;
```

```

*Proc PLOT data=can;
*plot can2*can1=cluster /vpos=30 hpos=60;
*run;

```

```

Proc CLUSTER data=yuma method=average pseudo std outtree=yumtree;
id Plot;
var Slope Val_w Rate_vw Perc_veg No_chan;
run;
Proc tree data=yumtree;
id Plot;
run;

```

```

*Proc PRINT data=yumtree;
*run;

```

```

Proc sort data=yuma;
by cluster;
run;

```

```

Proc means data=yuma;
var Net_ch RScour RFill Thal_ch Slope Val_w Rate_vw Bedrock No_chan
Q V Shear Power UPower WD
Perc_veg Wat_wid Wet_A Avg_d Mx_d ;
by cluster;
id Plot;
title 'CLUSTER MEANS';
run;
Proc sort data=yuma;
by SF;
run;

```

```

Proc means data=yuma;
var Net_ch RScour RFill Thal_ch Mx_d Slope Val_w Rate_vw No_chan;
by SF;
run;

```

```

*Proc STEPDISC data=yuma;
*class cluster;
*var Slope Val_w Rate_vw Bedrock No_chan;
*title 'Stepwise Discriminant by Cluster';
*run;

```

```

Proc STEPDISC data=yuma;
class SF;
var Slope Val_w Rate_vw Perc_veg No_chan
Wat_wid Wet_A Avg_d Mx_d V Q Shear Power;
title 'Stepwise Discriminant by SF';
run;

```

```

*Proc DISCRIM data=yuma method=normal pool=yes manova wcov pcov list out=cout;
*priors equal;
*class cluster;
*var Slope Val_w ;
*id Plot;

```

```
*title 'Discriminant by Cluster';  
*run;
```

```
Proc DISCRIM data=yuma method=normal pool=yes manova wcov pcov list out=cout;  
priors equal;  
class SF;  
*var WD No_chan;  
var Val_w No_chan;  
*var Mx_d;  
id Plot;  
title 'Discriminant by Scour/Fill';  
run;
```

```
Proc DISCRIM data=yuma method=normal pool=yes manova wcov pcov list out=cout;  
priors equal;  
class SF;  
id Plot;  
*var Mx_d Slope;  
*var Mx_d Slope Perc_veg;  
var Mx_d;  
title 'Discriminant by Scour/Fill';  
run;
```

**List of all participating scientific personnel**

Dr. Ellen E. Wohl, Associate Professor of Geology, Dept. Of Earth Resources, Colorado State University

David M. Merritt, PhD candidate, Dept. Of Earth Resources, Colorado State University